Pergamon

0301-9322(94)E0017-D

Int. J. Multiphase Flow Vol. 20, Suppl., pp. 169–209, 1994

0301-9322/94 $26.00 + 0.00

PREFERENTIAL CONCENTRATION OF PARTICLES BY TURBULENCE

J. K. EATON and J. R. FESSLER

Department of Mechanical Engineering, Stanford University, Stanford, CA 94305, U.S.A.

(Received 18 February 1994)

Abstract—Preferential concentration describes the accumulation of dense particles within specific regions of the instantaneous turbulence field. This phenomenon occurs in dilute particle-laden flows with particle time constants of the same order as an appropriately chosen turbulence time scale. The mechanisms which drive preferential concentration are centrifuging of particles away from vortex cores and accumulation of particles in convergence zones. Experimental and numerical studies are reviewed which demonstrate that preferential concentration occurs in a wide range of flows including plane and axisymmetric free shear flows, wall-bounded flows, homogeneous turbulent flows, and complex shear flows. The same basic mechanisms are active in all these flows but the specific effects and the definition of an appropriate time scale change from problem to problem. Preferential concentration has been shown to have a significant effect on droplet combustion, aerosol particle settling and turbulence modification by particles and is expected to be significant in numerous other applications. Current models describing preferential concentration and its global effects on the flow are inadequate.

Key Words: particle concentration field, particle clustering, turbulence, particle laden flow, droplet clustering, particle–vortex interaction, particles

1. INTRODUCTION

Turbulent flows laden with solid particles or liquid droplets are a common occurrence in both nature and technology. The interaction between the particles and the turbulence often plays an important role in determining the performance of engineering devices. Accurate modeling of the particle motions is needed to design new or improved products and also to help reach decisions in such matters as mitigation of environmental impacts. Recent research has shown that the particle concentration in turbulent flows may be highly non-uniform with local regions of anomalously high or low concentration. The variations in particle concentration are far greater than would be expected from statistical considerations. This raises serious concerns about the utility of statistical models to represent particle-laden turbulent flows. Once we understand the mechanisms for preferential concentration, we also must ask if we can control and/or make use of the non-uniformity in the concentration field.

The term preferential concentration means that the instantaneous particle concentration field is correlated to the turbulent motions. Regions of either high or low particle concentration may be associated with specific turbulent structures or may have been formed by the action of turbulent eddies over a short time preceding the observation. This phenomenon goes by several different names including particle clustering, inertial-bias, local accumulation, self organization, directed motions and de-mixing but in each case the same basic mechanisms are involved.

Our developing understanding of preferential concentration must be contrasted with conventional theories of particle dispersion. Such theories treat the turbulence in a purely statistical sense as a source of random forcing applied to the particles. The earliest such treatment was developed by Taylor (1921) and has been refined by many workers culminating with the recently published work of Mei *et al.* (1991). The statistical theories treat particle dispersion much like the diffusion of a passive contaminant. Often, a turbulent diffusivity is calculated based on the properties of the turbulence and of the particles. These theories always predict that particles will diffuse away from a point source and that particles which are initially uniformly distributed in a turbulent field will remain uniformly distributed in the absence of body forces.

The statistical theories of particle dispersion ignore the wealth of modern research on turbulence which shows that the turbulence is dominated by quasi-deterministic coherent structures. The

coherent structures are vortical elements characteristic of a specific flow. Coherent vortical structures were first observed in simple shear flows like the plane wake and the plane mixing layer where the basic instability produces large scale vortices which are essentially two dimensional. Coherent structures have also been identified in wall-bounded flows where the turbulence is fully three dimensional. Close to the wall, the turbulence is dominated by longitudinal vortex elements while in the wake region arch-shaped vortices are predominant (see the extensive review by Robinson 1991). Even homogeneous flows such as grid turbulence have been observed to have characteristic vortical structures (c.f. Rogers & Moin 1987; Ruetsch & Maxey 1992). For example, Ruetsch & Maxey found that the intense vorticity fluctuations in homogeneous, isotropic turbulence are concentrated in tube-like structures. The available evidence (described later in this paper) indicates that the coherent structures may be modified by the presence of particles but they are still present in the same basic form for mass loading ratios (mass of particles/mass of fluid) up to unity. There is no definitive proof to date but, these structures may remain important up to even higher loading.

The coherent vortical structures are the mechanisms that cause preferential concentration by producing directed (non-random) motions of particles. This is most often seen in gas flows laden with solid or liquid particles where there is a large density difference between the particles and the carrier fluid. The dense particles cannot follow the instantaneous fluid flow streamlines so an individual particle does not necessarily remain with a given fluid element. To understand how this may result in preferential concentration we consider the two simple two-dimensional flows illustrated in figure 1. The picture at the bottom shows a particle moving in the neighborhood of a two-dimensional vortex. The particle cannot follow the curved streamlines and instead spirals away from the center of the vortex. Therefore, we expect to find that vortex cores would be regions of low particle concentration; an expectation that has been confirmed by numerous experiments and simulations as discussed below. The picture at the top shows a region of converging flow. This region is characterized by high strain rate and low vorticity. As before, we see that a typical particle entering this region crosses curved streamlines. In this case, we expect to find a high concentration of particles in the central region and this expectation is again borne out by experiment and simulation. Of course, the real situation is much more complicated than the one described above. The actual coherent structures are evolving in time

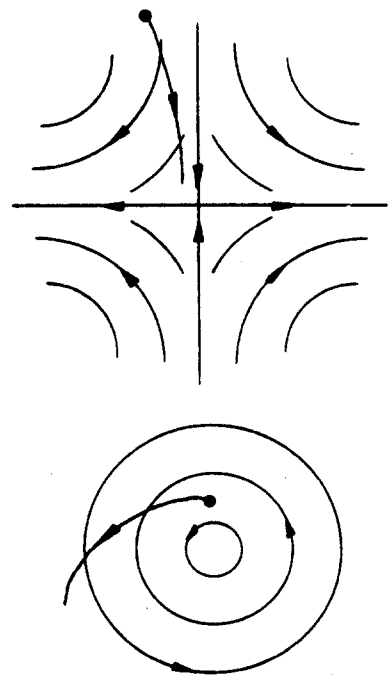

Figure 1. Particle interaction with simple two-dimensional flows.

and in many real flows they are fully three dimensional. At reasonably high Reynolds number, many different scales of motion may be superimposed. The particle characteristics are also important. For example, a very small particle might follow the flow streamlines precisely. Indeed, laser-Doppler velocimetry and particle-image velocimetry depend on this. The particles may also have a body force induced mean drift through the turbulent field.

Despite the complexities mentioned above, preferential concentration has now been observed in many different flows. The purpose of this paper is to describe the many experiments and numerical simulations that have revealed preferential concentration pointing out the similarities and differences in research approach and in the results. Crowe *et al.* (1988, 1993) have presented detailed reviews of particle motions in free shear flows. We have examined a wider class of flows to ascertain if the findings in cases with relatively simple vortex structure can be generalized to more complex flows. We have also added comments on how preferential concentration may affect turbulence modeling and speculation on the types of models that may be needed to capture this important effect.

We focus here on a particular class of particle-laden flows, namely dilute dispersions of fine particles (or droplets) in a turbulent flow field. We are interested in cases in which the particle volume fraction is small so that particle–particle interactions are rare and an individual particle's motion is determined only by its interaction with the fluid phase. We further restrict our attention to cases in which typical particle diameters are less than or at most equal to the smallest length scales of the turbulence motion. Thus, the turbulent fluid flow should be quite similar to an equivalent single phase flow; having similar turbulence levels and an eddy structure determined by the boundary conditions and not by the motions of particles. In such flows the dense regions or voids in the particle distribution are formed by the action of the turbulent eddies on the individual particles. Even within the restrictions stated above, the particles may still carry a significant fraction of the mass and momentum in the system and the particles acting collectively (but not individually) may modify the fluid mean velocity and turbulence field.

The restricted class of particle laden flows does not include cases in which the particle motions are controlled largely by interparticle collisions. Such flows may also form strong concentration inhomogeneities but by entirely different mechanisms. We also ignore flows carrying large particles with particle diameters on the same order as flow length scales. In such flows, each individual particle creates a significant disturbance in the flow field and particle clusters may form driven by the interaction of the individual particle disturbance fields (c.f. Tory *et al.* 1992). Despite these omissions, our restricted class still includes a large number of natural and technologically important flows. Examples of flows within the present regime of interest include pulverized coal combustors, fast fluidized beds, dust and rain storms and spray burners. Most such flows involve the motion of particles or droplets in a gas flow and indeed most of the examples discussed below are for such cases. However, some important cases have been observed in solid–liquid systems and a few of these will be discussed here. Some problems in bubbly flows also offer important similarities but they will not be surveyed here. Many of these problems can be addressed by similar research techniques as particle-laden flows (c.f. Ruetsch & Meiburg 1993). Most of the papers we have examined are those in which the specific point of the research was to examine particle motion in a turbulent flow. We suspect that there are many more flow visualization studies that have shown evidence of preferential concentration.

2. THE ROLE OF THE STOKES NUMBER

The Stokes number is defined as the ratio of the particle aerodynamic time constant to an appropriate turbulence time scale. The central role of the Stokes number in determining the effects of turbulence on a particle's motion has been pointed out in the review of Crowe *et al.* (1988) and by many others. For a particle moving in a uniform flow at Reynolds numbers much less than one, the particle time constant is:

$$\tau_p = \frac{(2\rho_p + \rho_f)d_p^2}{36\,\mu},$$

In the case of particles which are much denser than the fluid this reduces to (Stokes 1851):

$$\tau_p = \frac{\rho_p d_p^2}{18\,\mu}.$$

While the assumptions of Stokes' analysis are violated for many of our flows of interest, the time constant calculation remains quite accurate for particle Reynolds numbers up to the order of unity. At higher particle Reynolds numbers, the time constant can be estimated using relatively simple drag laws such as the one proposed by Oseen (1927) valid for particle Reynolds number up to 200:

$$C_D = \frac{24}{\mathrm{Re}_p}[1 + 0.15\mathrm{Re}_p^{0.687}],$$

In certain simple turbulent flows the choice of the turbulence time scale is obvious. However, it is frequently quite difficult to select an appropriate turbulence time scale and this will be discussed further below. Table 1 gives a selection of flows and particles to give the reader an idea of the range of Stokes numbers in typical applications.

The most well known occurrence of preferential concentration is the very low particle concentration found in the cores of strong vortices for gas flows carrying solid particles. In many cases the vortex core is completely devoid of particles and there is a halo of particles surrounding the vortex. This seems like an obvious effect until it is pointed out that it occurs only at intermediate Stokes numbers. In order to understand this, consider a simple flow in which both the fluid and randomly distributed particles are initially at rest. A Rankine vortex suddenly appears in the flow at time zero. We will follow the motion of various size particles moving around this vortex. First though, it is noted that this is a rough model of what actually happens in turbulence. A vortex sheet may roll up into an intense vortex or a vortex tube may be stretched intensifying the vortex. The vortex formed by either of these mechanisms will eventually either diffuse away or more likely be grossly distorted by other turbulent motions.

Returning to the simple two-dimensional flow, it is assumed that the vortex remains steady for some time following the impulsive start. The vortex has a core radius of r_0 and a tangential velocity at the edge of the core of V_0. An appropriate time scale for this eddy is then r_0/V_0 and the Stokes number is $\tau_p V_0/r_0$. A simple computer code was developed to track the motion of various size particles in the vortex. The paths of two particles, one a fluid point and one a particle with Stokes number of 1, are shown in figure 2. Both were released at the same point at a radius of half the core radius. The fluid point follows a circular streamline as expected. The heavy particle moves slowly at first then follows a spiral path moving quickly out of the vortex core. Figure 3 quantifies this effect for a wide range of Stokes numbers. The figure shows the particle's radial position after 3 and 6 fluid time scales. We see that particles with a Stokes number less than about 0.01 remain at nearly constant radius. These particles follow the flow and would not be preferentially concentrated. The same is true for particles with Stokes numbers greater than 25 although this case is a little more difficult to understand. These heavy particles are so slow to respond that they just barely begin to move in the period shown here. In the real situation, particles have only a finite time to interact with an eddy, so slowly responding particles are not preferentially concentrated.

The particle response to the vortex motion is most dramatic for Stokes numbers between 0.1 and 1. We will see that preferential concentration is most frequently observed in the laboratory in exactly this same range. Unfortunately, the specification of the appropriate fluid time scale is not easy even for this simple flow. Another time to consider is the time it takes the eddy to decay. By 6 fluid time scales the vortex core will have made nearly one full revolution. By this time it is likely that the vortex would have either diffused significantly or would have been distorted by other vortices in the field. Therefore, an eddy lifetime may be an appropriate time to consider as a fluid time scale. There is a third time to consider if the particles have a significant mean velocity relative to the turbulent eddies; that is the time it takes a particle to traverse an eddy. If a particle with a Stokes number around 1 is dragged rapidly through an eddy (say by a body force field) it may feel little effect of the eddy. While the specification of the turbulence time scale is indeed difficult the basic conclusion remains the same. Particles with time scales on the same order as the fluid time scale will respond strongly to vortex motions and may be preferentially concentrated. Particles which are much lighter will follow the flow and remain in the vicinity of the same fluid element

Table 1. Stokes numbers for various flows and particles

	2 μm kerosene droplet $\tau_p = 10\ \mu$s	10 μm water droplet $\tau_p = 300\ \mu$s	28 μm Lycopodium $\tau_p = 1.7$ ms	50 μm glass sphere $\tau_p = 18$ ms	70 μm copper sphere $\tau_p = 95$ ms
Axisymmetric jet					
$D = 5$ cm, $U_j = 20$ m/s, $x/D = 5$,					
$\tau_f = 5$ ms	0.002	0.06	0.34	3.6	19
Mixing layer					
$\Delta U = 3$ m/s, $\delta = 10$ cm,					
large eddy time scale $\tau_f = 33$ ms	0.16	4.8	27.4	290	1500
Fully developed pipe flow					
$D = 10$ cm, $U_m = 10$ m/s					
viscous time scale $\tau_f = 62\ \mu$s	0.0059	0.18	1	11	56
Kolmogorov scale $\tau_f = 1.7$ ms	0.001	0.03	0.17	1.8	9.5
large eddy scale on cl $\tau_f = 10$ ms	0.00030	0.0091	0.052	0.55	2.9

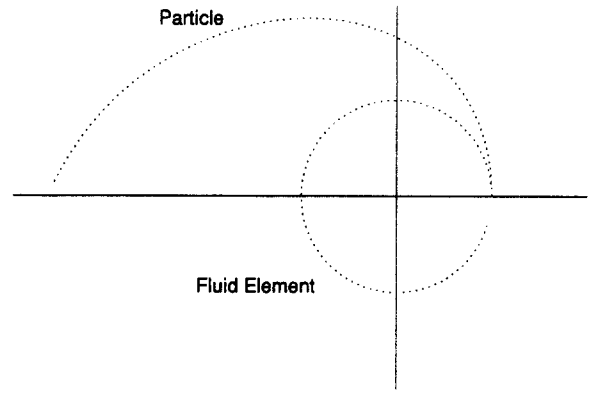

Figure 2. Pathlines of fluid element and particle with a Stokes number equal 1. Both are released from the same location in a Rankine vortex at a radius 1/2 that of the core.

for a long time. Such particles cannot be preferentially concentrated. Very heavy particles cannot respond to the vortex motion in the time available and will also not be preferentially concentrated.

3. REVIEW OF PREFERENTIAL CONCENTRATION STUDIES

This section reviews previous analyses, numerical simulations and experiments that have cast light on preferential concentration. The section is divided into subsections which group the studies by type of flow, including free shear flows, wall bounded flows, homogeneous flow and a catch-all category called complex flows which covers mostly complex jets and separated flows.

3.1. Free Shear Flows

Much of the early evidence on the influence of large-scale vortical structures on the particle concentration field was provided by studies of free shear flows. Crowe *et al.* (1988) reviewed numerous studies from the 1960s and 1970s which showed that the dispersion of particles in a free jet is greater than that for fluid particles. The studies investigated liquid droplets in air as well as solid particles in both air and water. Some of the investigators attributed the increased dispersion to the centrifuging of the particles by the large-scale vortices while others hypothesized that other factors such as injecting the particles with lateral velocity and Magnus lift forces were the cause. In a work by Yule (1981), the author claims to have direct photographic evidence of the interaction

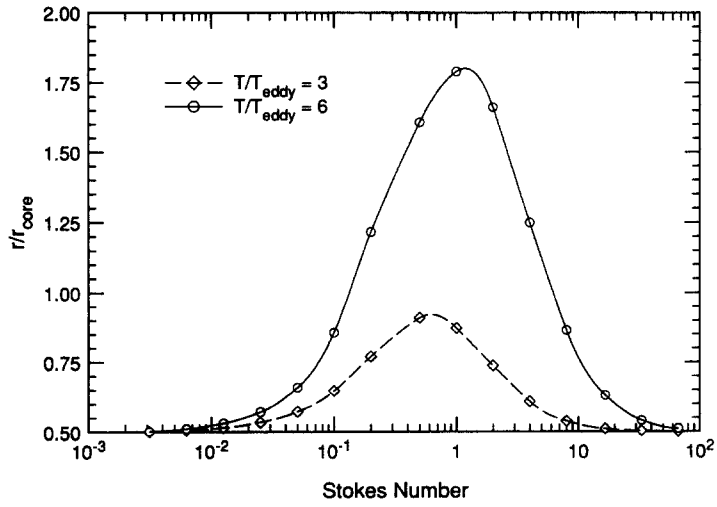

Figure 3. Radial position vs Stokes number for various sized particles released in a Rankine vortex at 1/2 core radius. $T_{eddy} = r_0/V_0$.

between particles and large-scale vortices. He states that small particles follow the gas flow and act as fluid tracers while larger particles are flung out of the vortices and penetrate the outer region of the jet. He further asserts that accurate modeling of particle dispersion must therefore necessarily take into account the interaction of particles with large-scale structures.

Since the research of Brown & Roshko (1974) we know that the behavior of free shear layers is dominated by large-scale vortices. Winant & Browand (1974) also showed that the growth of the layer is controlled by the pairing of the same signed vortices into a single, larger vortex. The shedding frequency and pairing behavior of these vortices can be controlled to produce a regular series of quasi-two-dimensional vortices. The regularity of these structures provides the perfect environment to study the interaction of particles with large-scale vortices. If particle mass loadings are small enough that they do not significantly affect the fluid flow properties, the location and flow characteristics of the vortices can be assumed known and the effect of the vortices on the particles is isolated. The ability to control the vortices also provides the opportunity to control the instantaneous particle concentration field.

The dominant role of these large-scale structures inspired Crowe *et al.* (1985) to study particle dispersion in a plane mixing layer by representing the layer as a series of Stuart vortices. The study showed reasonable agreement with previous experimental studies which showed that very small particles follow the flow and disperse as fluid particles while larger particles either disperse more or less than fluid elements. They also postulated that the relevant parameter for gauging particle dispersion is the Stokes number, the ratio of the particle response time to some time scale in the flow. Their results showed maximum dispersion for Stokes numbers on the order of 0.1. Particles with Stokes numbers less than 0.001 dispersed essentially as fluid elements while those with Stokes numbers greater than 1.0 showed much less dispersion. This simple model provided further evidence that large-scale vortices are in fact dominating particle dispersion in the plane mixing layer and established the Stokes number as the relevant parameter for non-dimensionalizing particle "size" when looking at particle dispersion.

The following section will review both experimental and numerical studies on preferential concentration in simple free shear flows including plane mixing layers, free jets and wake flows. It will concentrate on those studies which show either instantaneous or time averaged concentration data that directly illustrate the interaction of particles with large-scale vortices. Much of the earlier material has been previously summarized in reviews on particle dispersion in free shear flows by Crowe *et al.* (1988, 1993).

3.1.1. Plane mixing layers

(a) Experimental studies. Photographic evidence of the interaction of particles with large-scale vortices has been provided by a number of researchers for plane mixing layers seeded with either solid particles or liquid droplets. Kobayashi *et al.* (1988) used a strobe to produce simultaneous flow visualization of the fluid and particulate phases by seeding the high-speed side of the mixing layer with dry ice mist and the low-speed side with 30 μm dia glass particles. The results show the particles initially passing unaffected through the small vortices just past the splitter plate but later stretching out into "fingers" as they interact with the larger scale vortices downstream. Particle Stokes numbers, based on an eddy turnover time τ_f, ranged from 8 at 6 cm to 1 at 30 cm downstream of the splitter plate. Note that the local Stokes number for a particle must necessarily change as the shear layer grows since the fluid time scale used for non-dimensionalization was:

$$\tau_f = \delta/\Delta U$$

where δ is the vorticity thickness and ΔU is the change in velocity across the layer. LDA measurements of the transverse particle velocities show a trend of increasing transverse velocity with increasing particle size for the three sizes investigated (2.6 μm water droplets; 30 and 52 μm dia glass particles).

Kamalu *et al.* (1988) used a laser sheet to produce flow visualization of 30–40 μm spherical glass particles which were seeded just above the splitter plate in the fast stream. These particles correspond to Stokes numbers in the range from 4 to 1 for the region visualized using the same definition of the fluid time scale as Kobayashi *et al.* (1988). The images show the particles clustered into thin rings which surround the large vortices in the flow, with very few particles found in the

vortex cores. Comparison of forced and natural flow shows that increased dispersion results when the flow is forced at a subharmonic of its most unstable frequency. LDA measurements of the transverse velocities showed opposite trends for particles and the fluid. Fluid particles tend to be drawn into the center of the layer from both sides while particles are flung outward from the layer. More visualization, covering a wider parameter space is provided by the same investigators in Wen *et al.* (1992). The study compares the dispersion pattern with natural flow to flow forced at either a fundamental or a subharmonic of the most unstable frequency. Subharmonic forcing stimulated pairing in the layer and increased the layer growth rate. Images of both natural and forced flow from this study are shown in figure 4. Results are also shown for particle seeding at two different locations in the fast stream. Visualization of the dispersion patterns for 10, 30 and 40 μm dia particles shows distinctly different behavior for the 10 μm particles as compared to the larger particles. The smaller particles with Stokes numbers on the order of 0.1 seem to be uniformly distributed throughout the vortex cores while the larger particles avoid the vortex cores. Additional results from this paper are discussed in the section on computational studies.

Lazaro and Lasheras (1989) used an array of atomizers to seed the high speed side of a mixing layer with approx. 20 μm dia water droplets. Visualization of the mixing layer with collimated light from strobes shows the spray being drawn into the low-speed side by the vortices soon after the

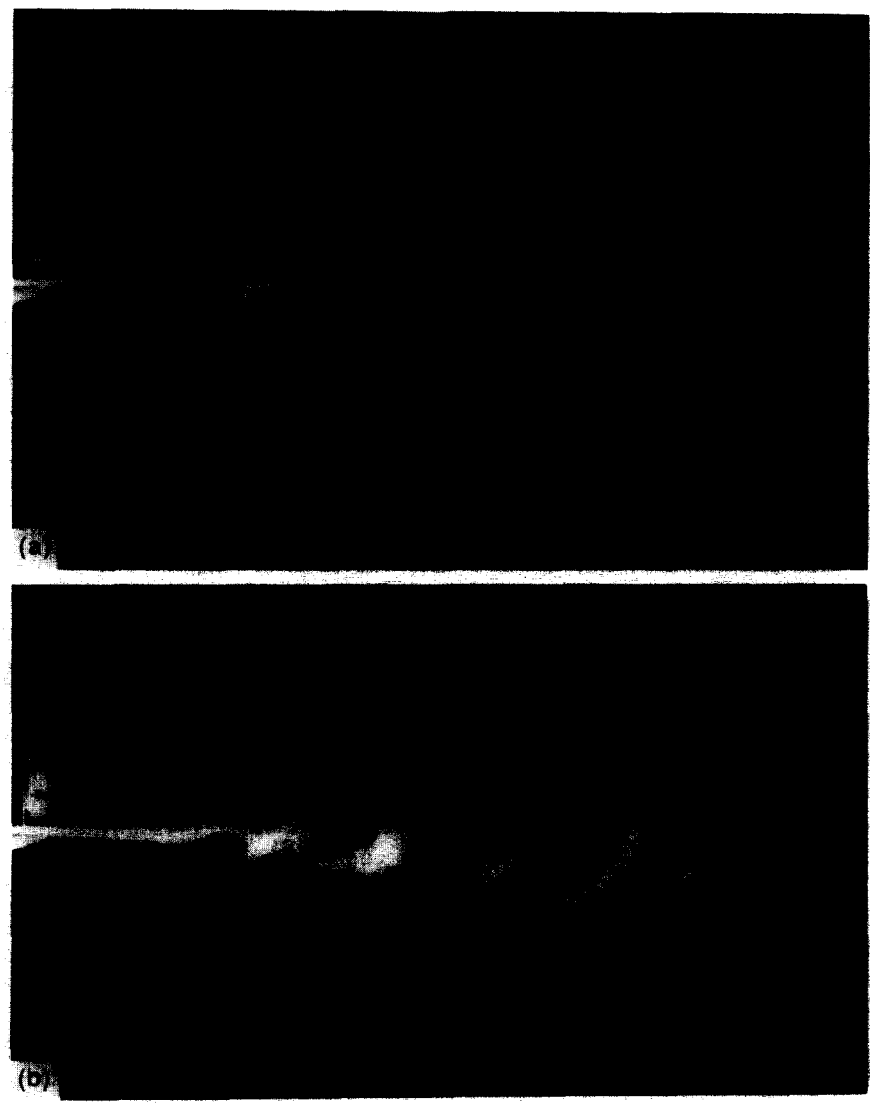

Figure 4. Dispersion pattern for 40 μm glass particles released in the fast stream of a plane mixing layer. $U_1 = 5$ m/s, $U_2 = 2$ m/s; (a) natural flow, (b) forced at first subharmonic of natural instability. Wen *et al.* (1992).

splitter plate. The regions corresponding to the vortex cores are almost completely devoid of particles. Measurements of the size distribution across the layer were taken at several downstream locations. These showed that the size distribution and the number density were not uniform across the layer. In fact, the layer was found to have three distinct regions: a core characterized by small mean droplet diameter which is surrounded by two layers with larger diameter droplets. Downstream, the mean diameter in the core continues to decrease as the larger droplets are flung out of the vortex cores.

Lazaro & Lasheras (1992a, b) extended this work and examined both the forced and unforced cases with the same experimental setup. For the natural case they found a universal collapse of the spreading rate for different sized particles when both the width of the layer and the downstream distance are non-dimensionalized by the following length scale:

$$L_D = (\rho_p/\rho_G)U_{inf}d_p^2/18v$$

where U_{inf} is a characteristic velocity scale. Laser attenuation measurements gave information about the temporal behavior of the layer. The droplet concentration fluctuations showed greater temporal coherence than fluid fluctuations, which is indicative of the droplet's strong response to the larger scales in the flow. Cross correlations of the concentration and fluid velocity show that the locations where the streaks of droplets extend into the low speed side of the layer correspond to the braid regions between successive vortices.

Interestingly the forced mixing layer showed some different characteristics from the natural layer. There is no universal collapse of the particle spreading rate as was found in the natural case. This is due to non-similarities in the gas layer growth due to the forcing. Phase averaged concentration measurements showed distinct streaks of high droplet concentration surrounding the vortex cores which are essentially devoid of droplets. These streaks were found to emerge further from the vortex core as the particle size is increased and the heavier particles are flung further out of the vortices. Also, a simple model of particle dispersion using a single isolated vortex was presented which showed good qualitative agreement with the experiments.

Ishima *et al.* (1993a) studied the effect of particle residence time in the layer on dispersion. Three different size classes (42, 72 and 135 μm glass beads) were injected into the gas flow at varying relative velocity to change their residence time within the layer. Particle concentration was measured by recording the rate of particles passing through an LDA measurement volume. The results indicate that increased relative velocity reduces the effect of the large-scale vortices on the particles due to smaller residence time within the vortex. Increasing the relative velocity was seen to have the same effect on dispersion as increasing the particle size which led to a modified Stokes number based on a fluid time scale, τ_f^*, which includes both the standard fluid time scale, $\tau_f = \delta/\Delta U$, and a characteristic residence time, $\tau_r = \delta/U_r$, where U_r is the relative velocity of the particle:

$$\tau_f^* = [1 - \exp(-A(\tau_r/\tau_f)^B]\tau_f$$

where A and B are experimentally determined constants given as 0.25 and 1.0, respectively. Collapse of the dispersion data was found for the three particle sizes and different injection velocities when using this modified Stokes number.

Glawe & Samimy (1993) extended the study of particle laden mixing layers to compressible mixing layers. They used flow visualization and image processing to study the dispersion of 5, 17 and 62 μm dia glass particles in mixing layers with convective Mach numbers, M_c, of 0.51 and 0.86. The $M_c = 0.51$ case showed much of the same trends as previous incompressible studies: a change in dispersion with Stokes number with maximum dispersion for the smallest particles with average Stokes numbers of 7. Similar results were not found for the $M_c = 0.86$ case and the differences were attributed to changes in the gas flow at higher convective Mach number. The gas flow structures in the higher compressibility case are more three-dimensional in nature and less organized. This effectively reduces the characteristic time scale for the structures and increases the Stokes numbers for the particles. As a result, no differences in dispersion were observed for the different Stokes number particles investigated.

(b) Numerical studies. The success of Crowe *et al.* (1985) in predicting particle dispersion using Stuart vortices and the experimental evidence of the role of large vortices in determining dispersion

suggests that fairly accurate computations of mixing layers can be accomplished using methods which take into account only the large-scale vortical motions. Numerical simulations also have several distinct advantages over experimental techniques in the study of particle laden flows. First, since the entire instantaneous flow field is known, direct correlations between the flow field and particle concentration field can be made. Second, a wider variety of particle Stokes numbers can be investigated without the physical constraints of finding appropriate particles. Finally, perfectly monodisperse, spherical particles can be simulated to eliminate any effects due to variations in particle size and shape.

Chein & Chung (1987) looked at the effect of vortex pairing on particle dispersion using a discrete vortex method. The discrete vortex method used in this case involves 96 small vortices arranged in four sinusoidal rows to simulate the interaction and pairing of only a single pair of vortices from the mixing layer. Rather than using point vortices which might produce unreasonably large velocities as two merge, vortex "blobs" are used, where each vortex has a finite sized smooth core. The mutual interaction of all of vortices defines the flow field and the vortices are allowed to freely translate throughout the field. The results of the study show a strong dependency of dispersion on particle Stokes number. Particles with very small Stokes numbers dispersed essentially as fluid elements while very heavy particles dispersed less than the fluid. For Stokes numbers in the range 0.5–5, the particles were found to disperse more than the fluid. Particle concentration profiles for these intermediate size particles showed distributions that are bimodal with low concentration in the center of the layer indicating that these particles are flung out of the vortices. The pairing behavior was also found to increase dispersion over what was observed for a single vortex before and after the pairing. The pairing process was found to be the primary mechanism for entraining particles back into the center of the layer from which they are subsequently ejected.

Chein & Chung (1988) extended this work to a spatially developing plane mixing layer. Again a similar discrete vortex method was used where at each time step a single vortex "blob" is shed from the tip of the splitter plate. Visualizations of the flow field exhibit similar growth and pairing behavior as seen in experimental studies. Particle dispersion is visualized by releasing streaklines of particles from two points above, two points below and one point right at the tip of the splitter plate. Results for six particle Stokes numbers, ranging from 0.1 to 500, are shown. Distinctly different behavior is observed for particles released on opposite sides of the plate. When released on the slow speed side of the layer, the Stokes number 1 and 10 particles look remarkably like the visualization shown in Kamalu *et al.* (1988) and Wen *et al.* (1992), with distinct rings of particles surrounding the particle-free vortex cores. Particles released on the high-speed side, on the other hand, do not penetrate the layer as well and show only fingers of particles extending down between the vortices, much like the results of Lazaro & Lasheras (1989) for droplets released on the high-speed side. The explanation for this different behavior is the difference in local Stokes number for the two sides of the layer. The dispersion results for this study show the intermediate size particles initially dispersing less than fluid particles but later exceeding the dispersion of fluid particles as they have time to interact with the vortices and the vortices have grown to larger scale.

Wen *et al.* (1992) use the same discrete vortex technique with a perturbation equivalent to acoustic forcing of a physical layer to directly compare numerical results to their experimental flow visualization. The results show streaklines for particles with Stokes numbers in the range 0.1–10 which have been released at various locations across the layer. Distributions of particle flux are bimodal with low flux at the layer center. A two part mechanism for particle dispersion is also suggested which involves "stretching" and "folding" of the particle clusters. The stretching mechanism involves particles which are thrown into the high-speed side of the layer by vortex action where the velocity gradient causes the cluster of particles to elongate and neighboring particles are rapidly separated. The folding process involves the pairing of successive vortices which each are surrounded by a ring of particles. As they pair the particles trapped between the two vortices are folded back into the center of the layer. Figure 5 shows two plots of instantaneous vorticity contours with particle locations which illustrate the stretching and folding mechanisms.

Tang *et al.* (1992) addressed the plane mixing layer by way of comparison to bluff body wakes. In an attempt to quantify what Stokes number particles show the maximum degree of preferential

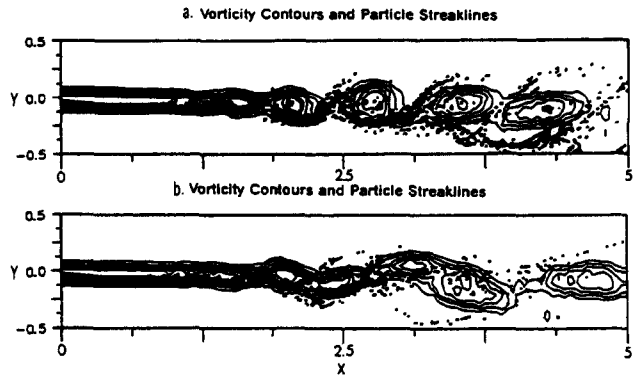

Figure 5. Instantaneous vorticity contours and particle locations from two-dimensional discrete vortex simulation of plane shear layer. (a) Stretching of particles clusters by velocity gradient on upper side, (b) folding of particles into layer by vortex pairing. Wen *et al.* (1992).

concentration, they introduced the concept of the fractal correlation dimension. This quantity, associated with chaotic systems, is defined as:

$$D = \lim_{l \to 0}(1/\log(l))\log(\Sigma(p_i^2))$$

where p_i is the probability that the distance separating two particles is less than some length l. This quantity will reach a minimum when all particles are clustered on a line and a maximum when they are uniformly distributed over space. Calculating the correlation dimension for the mixing layer study of Wen *et al.* (1992) shows a minimum for Stokes number of one, which agrees with the visual observations.

Samimy & Lele (1991) looked at particle dispersion in a compressible mixing layer. As opposed to the discrete vortex methods described earlier, they used a direct numerical simulation of the two-dimensional Navier–Stokes equations for temporally evolving mixing layers with M_c between 0.2 and 0.6. Particle dispersion was found to be maximum for particle Stokes numbers on the order of 1. As these results agree well with experimental and numerical results for incompressible mixing layers, compressibility does not seem to have much effect for $M_c < 0.6$. Compressibility may have more effect, however, for larger M_c, as shown by the experimental results of Glawe & Samimy (1993), or for larger Stokes numbers where the Mach number based on relative velocity is not so small.

Ganan-Calvo & Lasheras (1991) investigated a periodic Stuart vortex flow with heavy, settling particles. Certain sized particles were found to be permanently suspended in the flow rather than sedimenting. The suspension results when the tendency of the particles to be flung out of the vortices is just balanced by their settling. Tooby *et al.* (1977) had developed an experiment which showed this exact case. Their paths through the periodic flow were found to be attracted to either a single periodic, quasi-periodic or chaotic orbit depending on particle size. Tio *et al.* (1993) extended this work to buoyant particles as well and found that they also can be suspended in the flow but by a completely different mechanism. Buoyant particles are suspended in the stable equilibrium points within the cores of the vortices while heavy particles are trapped in a thin layer above the vortices.

Wang (1992) takes the novel approach of attempting to control particle concentration through non-uniform seeding of particles. It has been shown above that initially uniformly distributed heavy particles will be thrown out of vortex cores and clumped together around the edges of the vortices, which results in highly non-uniform distributions of particle number density. Some applications such as combustion, however, may benefit from more uniform particle distribution. To investigate this, Wang seeds a temporally evolving mixing layer simulation with fluid particles distributed non-uniformly in space. Note that this process is equivalent to seeding a spatially evolving layer non-uniformly in time. Certain non-uniform initial distributions can result in drastically more uniform distributions at later times. Although this study involved non-diffusive fluid tracer particles, the technique could also be applied to different density particles.

In summary, the interaction of particles with large-scale spanwise vortices in plane mixing layers is now well understood. Simple models representing only the largest vortices in the flow do an excellent job of replicating experimental results. The major physical mechanism is the centrifuging of particles away from vortex cores. Surprisingly, the effects of braid vortices on the concentration field have not been examined. These are intense vortices which are stretched and amplified by the strain field between the spanwise vortices (Bernal & Roshko 1986; Lasheras *et al.* 1986 and others). It seems likely that preferential concentration would occur for smaller particles than those most affected by the spanwise vortices. Visualization with a light sheet oriented normal to the flow direction would be worthwhile in this case.

3.1.2. Wake flows

Wake flows differ from plane mixing layers in that the vortices shed from the bluff body alternate in sign. As a result, pairing, as found in the mixing layer, is rare and growth of the layer is due to entrained fluid from the free stream surrounding the wake. Large-scale vortices do, however, dominate the flow structure so these flows also are ideal for studying preferential concentration due to large-scale organized structures. Early studies of particle laden wake flows were mainly concerned with the impact of particles on the body itself and the resulting erosion. Laitone (1981), however, continued to follow the particles that escaped impact as they interacted with the wake behind a cylinder. This study also involved a discrete vortex method with alternately signed vortices being shed from opposite sides of the cylinder. Large-scale vortices were represented by an agglomeration of smaller vortex "blobs". One plot is shown which superimposes the vortex blobs with the location and velocity of particles with $St = 1$. The particles essentially line the edges of the large agglomerations of vortex blobs with some penetration between successive vortices. Few particles are seen within the wake as they all came from upstream of the cylinder and must necessarily start outside the shear layer. As there is no pairing process to cause "folding" of the particles into the layer, they remain primarily on the edges of the vortices.

Chein & Chung (1988) studied the impingement of particles on normal and inclined plates using a discrete vortex method. Particles released upstream of the plate which do not impact the plate showed the same tendencies as seen in the study of Laitone (1981). For Stokes numbers from 1 to 25 the particles remain on the outside of the vortices as their inertia prevents them from entering the cores. Particles introduced behind the plates, however, begin to show signs of preferential concentration and dispersion was found to be inversely proportional to particle Stokes number. It was also found that increasing the initial injection velocity of the particles had the same effect as increasing the Stokes number of the particles. This effect was also noted in the experimental plane mixing layer experiments of Ishima *et al.* (1993) in which a modified Stokes number is introduced to take into account the residence time of particles in the layer.

Tang *et al.* (1992) performed an experimental and numerical study of the particle laden wake behind a bluff body. For the studies, particles are introduced at the end of the body into the wake region. Figure 6 shows the dispersion patterns in the numerical study for Stokes numbers from 0.01 to 100. Note that the $St = 0.01$ particles mark the fluid elements while the $St = 100$ particles pass through the layer only slightly affected by the large vortices. The numerical results bear a striking similarity to the experimental work which shows $St = 2.0$ glass particles in the wake illuminated with a laser sheet. As described above in the section on mixing layers, the study also introduced the fractal correlation dimension as a measure of the degree to which particles are preferentially concentrated on the edges of the vortices. As in the mixing layer study, a minimum correlation dimension of nearly 1.0 was found for $St = 1$ particles, which indicates a very high degree of organization.

Yang *et al.* (1993) used a laser sheet and strobes to visualize 10 and 30 μm glass beads ($St = 0.14$ and 1.33, respectively) in a bluff body wake flow. A photograph of the 30 μm beads with laser sheet illumination is shown in figure 7. The photograph visualizes a region from 2.5 to 7 body widths downstream of the body. Note how well the particles define the edges of the vortices in the flow. Quantitative number density distributions were obtgained with a technique similar to that of Longmire & Eaton (1992) in which the photograph is digitized and individual particles are identified and placed on a regular grid.

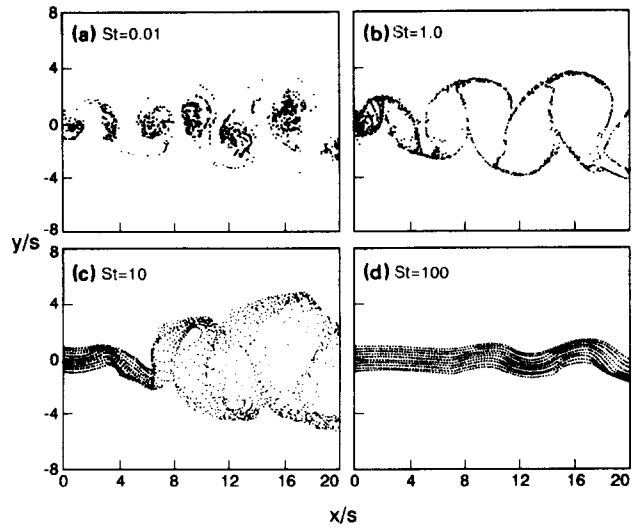

Figure 6. Instantaneous particle locations from two-dimensional discrete vortex simulation of plane wake. Particles introduced in the wake behind bluff body. (a) St = 0.01, (b) St = 1.0, (c) St = 10, (d) St = 100. Tang *et al.* (1992).

Bachalo *et al.* (1993) also report seeing voids and clusters of water droplets in the wake behind a cylinder. Using a phase-Doppler anemometer they were able to provide fluid and droplet velocity information as well as time of arrival data for the droplets. Spectral analysis of the time of arrival data showed a peak in the spectrum at a frequency corresponding to the dominant frequency of vortex shedding from the cylinder. As they point out, however, the time of arrival data for droplets is directly proportional to the droplet velocity so a correlation to the fluid velocity field would be expected. To eliminate this dependence, they calculate the droplet number density by dividing the data rate by the droplet velocity and measurement volume cross-sectional area. Cross correlations of the number density and fluctuating fluid velocity show very strong periodicity. This indicates that the droplet concentration field is strongly correlated with the periodic flow field.

Ishima *et al.* (1993b) investigated the particle laden flow field behind a pair of cylinders. The cylinders were separated by a distance of either 0.3 or 2 dia on a line perpendicular to the flow

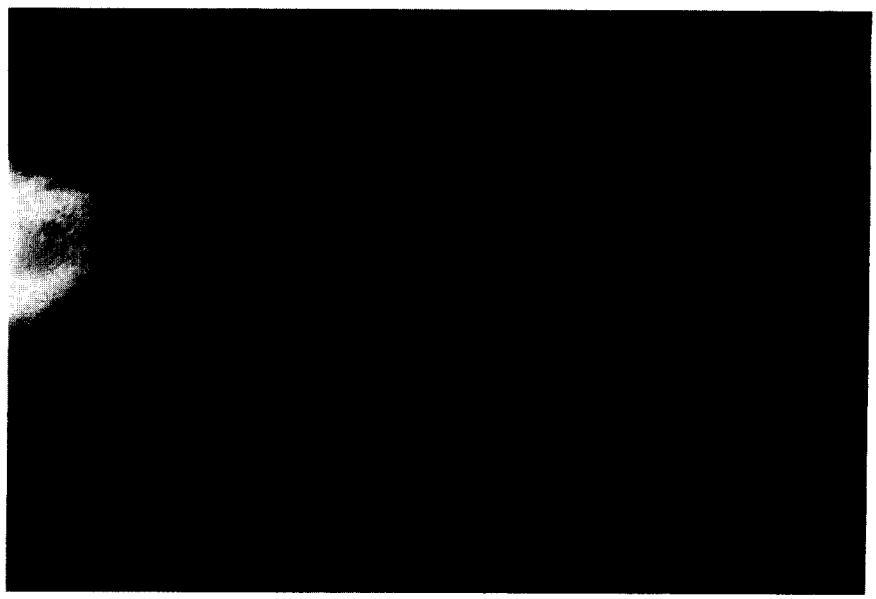

Figure 7. Single laser pulse flow visualization of 30 μm glass particles in a plane wake behind the bluff body. Yang *et al.* (1993).

direction. Particles were seeded into the flow along a splitter plate upstream and between the cylinders. For the case with smaller separation distance, the location of maximum particle number density was found to change with downstream distance as the particles interacted with the vortices from both of the cylinders. For the case with larger separation, however, there was no interaction with the vortices and the location of maximum number density remained on the centerline between the two cylinders.

3.1.3. Jet flows

As stated above, much of the early evidence of preferential concentration was provided by studies of particle spreading rates in jet flows. Significant effort has been expended on jet flows because they are so commonly found in industrial processes ranging from sprays to coal combustors. Like the other free shear flows reviewed above, axisymmetric jet flows provide ample opportunities to investigate the interaction of heavy particles with large-scale vortices. The near field of a jet can be thought of as an axisymmetric mixing layer, as the flow is dominated by a series of large vortex rings which translate and merge much like the spanwise vortices in a mixing layer. Further downstream, however, a helical mode begins to dominate the flow and much of the coherence of the vortical structures is lost. As a result, most of the work performed has concentrated on the near field where the vortices are largely two-dimensional in nature and particle interactions with discrete vortices can be identified.

Chung & Troutt (1988) used a discrete vortex method involving axisymmetric vortex rings to simulate a spatially developing jet. Simulated particles with Stokes numbers ranging from 0.05 to 100 were introduced to the flow a short time after the jet start-up in a region near the pipe wall. The fluid time scale used for non-dimensionalization was:

$$\tau_f = D/U_0$$

where D is the initial jet diameter and U_0 is the velocity in the jet core. The results showed a strong dependency on particle Stokes number with $St = 0.05$ particles acting as fluid tracers while the $St = 100$ particles passed through the domain with only slight perturbations due to the vortices. The $St = 1$ particles showed maximum dispersion as they ringed the large-scale vortices and less effect was seen for the $St = 10$ particles where "fingers" of particles were drawn out from the jet. Particles released closer to the jet centerline showed less dispersion and preferential concentration than those released near the pipe wall. These particles remained in the core region longer and as a result were less likely to interact with the vortices in the shear layer. In fact, the Stokes number for maximum dispersion was shifted to much lower values for particles released near the centerline.

Longmire & Eaton (1992) performed an extensive experimental investigation of a particle laden jet with Reynolds numbers on the order of 20,000. Their work included phase-averaged and instantaneous flow visualization of the fluid and particle phases as well as phase-averaged LDA measurements of particle velocity. The jet was acoustically forced with an audio speaker at various frequencies corresponding to Strouhal numbers (fD/U_0) between 0.26 and 1. The fluid time scale used to compute Stokes numbers was defined as the distance between successive vortices divided by their convection velocity taken as one half the jet core velocity. Although only a single size of particles (55 μm glass) was investigated, the effective Stokes number could be changed simply by changing the forcing frequency. The change in forcing frequency also changed the strength of the vortices. Phase-locked flow visualization of the fluid and particle phases shows distinct and repeatable particle clusters occurring in the highly strained region just downstream of the large vortex rings (figure 8). Particles were pulled from the clusters by the outward-moving flow at the downstream edge of the vortex rings. Maximum preferential concentration was found for Strouhal numbers around 0.5 which corresponds to Stokes numbers on the order of 5. This was the lower bound of Stokes numbers investigated so greater preferential concentration may have been found for lower Stokes numbers.

Particle number density distributions were obtained by digitizing 25 instantaneous photographs of a specific phase in the forcing cycle. The contour plots shown in figure 9 illustrate the important aspects of the concentration field. In the Strouhal number = 0.51 case there are distinct clusters of high particle concentration separated by strands of lower concentration. The regions which correspond to the vortex cores are devoid of particles. The Strouhal number 0.9 case shows almost

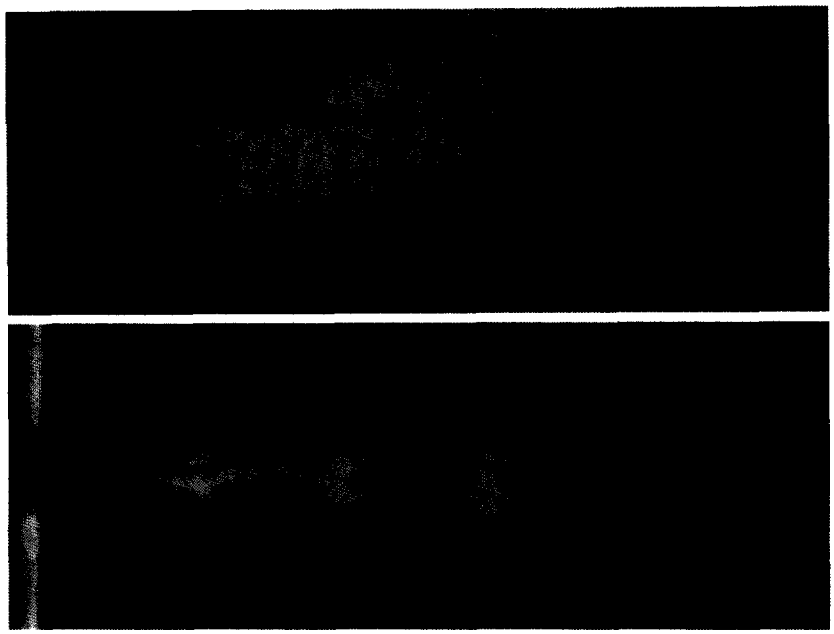

Figure 8. Phase-averaged flow visualization of single phase and particle-laden acoustically forced axisymmetric jet flow, 55 μm glass particles, Strouhal number = 0.43, $Re_D = 23{,}000$. Longmire & Eaton (1992).

none of these features because the fluid structures are smaller which results in larger effective Stokes numbers for the particles.

The flow was also forced with a combination of a fundamental and a subharmonic frequency to induce pairing. The particle clusters were found to pair along with the fluid structures creating larger particle clumps which are then dispersed widely in both the axial and radial directions. Phase-locked velocity measurements confirmed that particle ejections from the jet occur in a certain region which lies between successive vortices. Most of the measurements were for relatively low particle mass loadings (5–11%) to facilitate individual particle identification but phase-averaged flow visualization for mass loadings up to 65% was also shown. Direct comparison of low and high loading cases showed similar particle structures so it was concluded that the gas phase structures persist for loadings up to 65%.

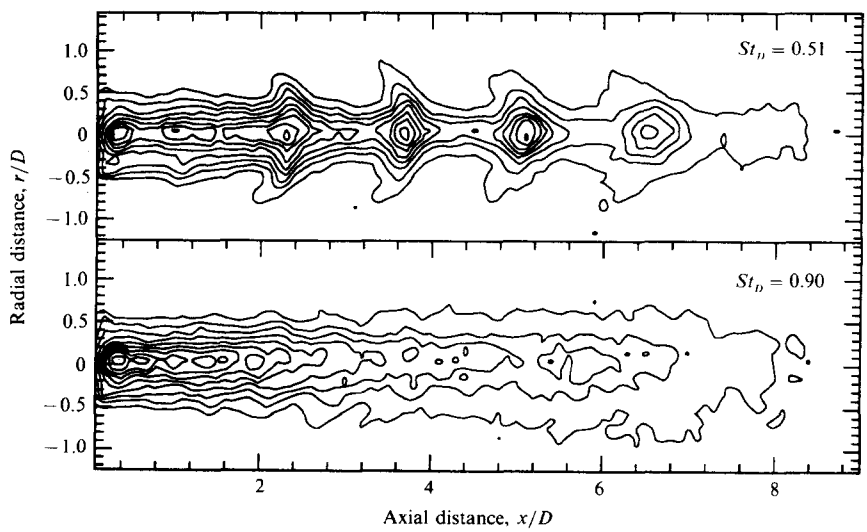

Figure 9. Phase-averaged particle number density maps for axisymmetric jet forced at a Strouhal number = 0.51 and 0.90. Longmire & Eaton (1992).

Hansell *et al.* (1992) performed both two- and three-dimensional simulations of the near field of a jet for three different particles with Stokes numbers from 3 to 38. The three-dimensional simulation used vortex rings which were periodically released from the jet exit with small helical disturbances. The investigation revealed a two-step mechanism for particle dispersion coupled to the pairing of vortices in the flow. In the first step, particles are left behind by a vortex as it accelerates to pair with a downstream vortex. These particles are stranded in the low-speed region between successive vortices until, in the second step of the process, they are flung out radially by the next passing vortex. For distances up to five jet diameters downstream, circumferential dispersion of particles was found to be negligible so the investigators concluded that in the near field, a two-dimensional simulation should be adequate. They also investigated the effects of high pressure and the relative importance of the Basset, virtual mass and buoyancy forces as compared to simple drag. Underprediction of radial dispersion was found when assuming only drag forces with the effect increasing with increased pressure and particle size.

Uthuppan *et al.* (1993) simulated a transitional jet (Mach number 0.57) with a finite difference solver of the two-dimensional Euler equations. The simulation models a 1.4 cm dia jet with $U_0 = 200$ m/s that was assumed to be initially laminar. The particles simulated correspond to water droplets with Stokes numbers from 0.02 to 53 based on the frequency of the second pairing in the flow. They found maximum dispersion for $St = 0.8$ and increased dispersion as compared to fluid elements for Stokes numbers between 0.1 and 4. Flow visualization of the near field shows the influence of the large-scale vortices on the dispersion of individual particles. They also emphasized the influence of the second pairing on dispersion. Particles of different size were found to follow similar paths through one pairing but were flung out in radically different directions after the second pairing. They, like Chung & Troutt (1988), found that only small particles released in the core were affected by the large-scale eddies while larger particles tended to remain in the core.

The results from the jet studies, perhaps not surprisingly, show qualitatively the same mechanisms as were found in the mixing layer studies. In the case of the jet though, the more important effect appears to be the formation of clusters in the highly strained regions rather than flinging of particles away from vortex cores. This may be because the particles never have an opportunity to enter the vortex cores. The jet studies also show great sensitivity to initial particle location and illustrate the strong effect that the pairing process has on radial dispersion. There seems to have been little study of the interaction of the jet far field with the particles. Although the structure is not so easily observed in the far field, there is still a dominant (helical) mode that is likely to produce variations in the concentration field of appropriately sized particles. There is also a possibility that clusters of particles formed in the jet near field may persist in the decaying turbulence of the far field.

3.2. Complex Shear Flows

Complex shear flows differ from simple free shear flows in that there is some factor, such as swirl or the presence of a wall, which makes the flow fully three-dimensional in nature. The presence of these complicating factors tends to make the flows studied more realistic but unfortunately more difficult to compute numerically. As a result, the few studies which are available for these types of flows are experimental. Unfortunately, the complex three-dimensional nature of these flows also makes the identification of coherent vortices, and thus preferential concentration, more difficult.

Swirling flows laden with droplets and heavy particles are of considerable interest to combustion engineers in particular, as swirl-stabilized combustors are commonly used in industry. The combustion aspects of these flows have been extensively investigated and early research is reviewed in Lilly (1977). More recently, numerous investigators have studied the fluid dynamics of swirling, particle-laden jet flows (Rudoff *et al.* 1989; Hardalupas *et al.* 1989; Sommerfeld *et al.* 1992) but the results are primarily statistical in nature and little information on the instantaneous concentration field is available. Rudoff *et al.* (1989) studied a small commercial swirl-stabilized burner with a phase-Doppler particle analyzer and flow visualization. Instantaneous images of the burning spray show intermittence in the flame which is indicative of non-uniform droplet dispersion. Clusters of drops and voids were also evident in the time of arrival data for droplets of water and non-reacting kerosene. Fast Fourier transform analysis of the time of arrival data showed peaks in the spectra for frequencies around 70 Hz. This frequency corresponds to Strouhal numbers for

the orifice surrounding the nozzle of about 0.25. These results led the investigators to postulate that the clusters of droplets were a result of interactions with vortices shed from the orifice. Clusters of droplets were also observed from time of arrival data by McDonell *et al.* (1992). This study of a spray with swirling atomizing air found evidence of particle clusters on the edges of the spray for the non-reacting flow of approx. 50 μm dia methanol droplets. The clustering was even more pronounced for the reacting case where distinct voids were observed in the spray. The authors could not conclude, however, whether the clusters resulted from the atomization process or from interactions with flow structures.

Currently Wicker & Eaton (1994) are studying the effects of acoustic forcing on particle dispersion in a swirling, co-flowing, particle-laden jet. In this flow particles are seeded into the core flow which is surrounded by a swirling annular flow. This configuration is similar to the complex flow field found in utility boilers. The flow configuration achieves swirl numbers sufficient for flow recirculation which results in a stagnation point in the flow about two inner jet diameters downstream of the jet exit. Smoke flow visualization of the single phase flow indicates that forcing the annular flow can result in organization of coherent structures similar to those found in single axisymmetric jets despite the flow field remaining highly three-dimensional. Figure 10 shows images of 90 μm glass particles illuminated by 25 laser pulses locked to a specific phase of the forcing frequency along with phase-averaged smoke visualization of the single phase flow. The particles stagnate just past the fluid stagnation point and are then flung outward by the swirling flow. Figure 11(a) and (b) shows contour plots of particle number density for the natural and forced cases, respectively. The contour plots were produced by scanning and averaging 25 images of a single laser pulse and identifying individual particles. Forcing changes the aerodynamic flow field by increasing growth rates in the jet near field which results in moving the location of the stagnation point closer to the jet exit. Comparison of figure 11(a) and (b) illustrates that forcing increases the spreading rate of the particles. The particles just downstream of the jet exit are flung farther from the jet centerline by the more coherent vortical structures in the forced flow. The shape of the contours is similar to those of Longmire & Eaton (1992) for a single round jet which show regularly spaced clumps of high concentration separated by regions of lower concentration. These similarities as well as comparison with single phase visualization indicate that the particles in the near field of this flow are being preferentially concentrated into the low vorticity, highly strained regions between coherent vortices. Particles are also concentrated near the stagnation point, a region of high mean strain.

The interaction of shear flows with solid surfaces also greatly complicates the flow field and therefore studies of preferential concentration. Longmire & Anderson (1993) studied a particle-laden round jet impinging on a flat plate five jet diameters downstream of the exit. Two sizes (30 and 20 μm) of solid, and one size (40 μm) of hollow glass particles were investigated for both natural and acoustically forced flow. The behavior of the jet prior to impingement is very similar to the behavior of the particle-laden free jet studied by Longmire & Eaton (1992). After impingement the coherent axisymmetric structures are seen to persist and expand radially along the plate. Figure 12 shows an instantaneous image of the flow seeded with both smoke and Stokes number 0.34 particles. The image clearly shows the clustering of particles between successive vortices both in the free jet and in the wall jet after impingement. Particles are also strongly concentrated near the stagnation point, a highly strained region of the mean flow. Forcing the flow was found to thicken the particle layer on the plate as the coherent vortices fling particles up into stagnant air above the wall jet. Figure 13 shows a view from below the glass impingement plate for forced flow. A distinct axisymmetric ring of particles is visible where the particles are clustered between two radially expanding vortex rings and voids are observed where the vortex cores are located.

Another wall-bounded shear flow of particular interest is the backward facing step or sudden expansion flow. The sudden expansion is frequently used in particle or droplet dump combustors as a flame holder. Hardalupas *et al.* (1992) studied particle dispersion in a vertical round sudden expansion with expansion ratios of 3.33 and 5. The particles investigated were 40 and 80 μm glass beads. Although they do not show any instantaneous flow visualization, they did find bimodal probability distribution functions for both radial and axial particle velocities in the shear layer when the large eddy Stokes numbers for the particles were of order one. These, along with increased

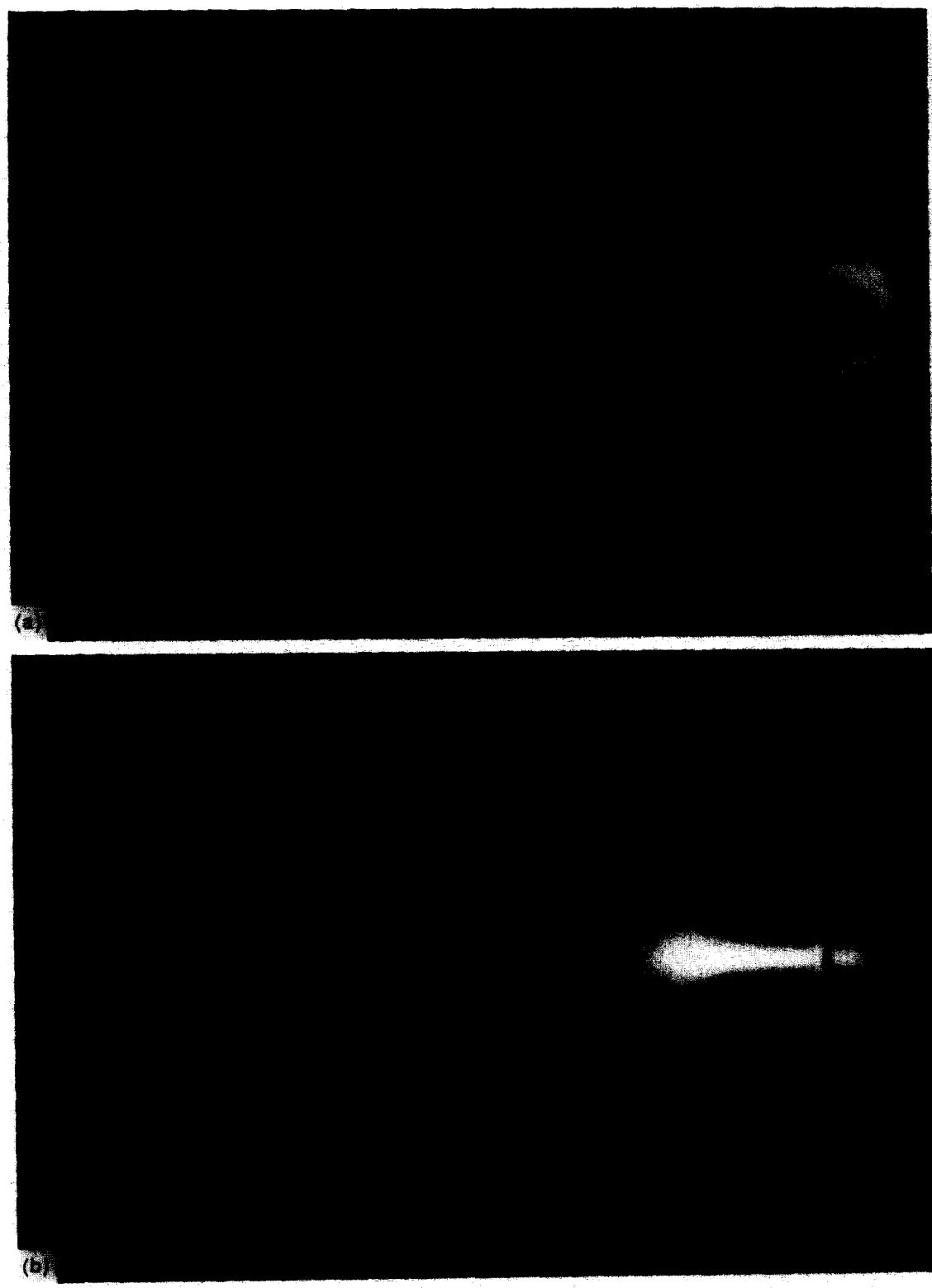

Figure 10. Flow visualization of a co-flowing, swirling jet with (a) smoke seeded in annular flow, (b) 90 μm glass particles in core flow. Photograph shows image of 25 superimposed laser pulses, phase-locked to forcing frequency of annular flow. Wicker & Eaton (1994).

measured particle velocity fluctuations, indicate that intermediate size particles are thrown into the recirculation zone by the vortices shedding off the step.

The results from the few studies on preferential concentration in complex shear flows show that the same types of mechanism that were evident in simple shear flows are still present. Particles are flung outward from the vortex cores and are collected in the highly strained region between vortices although they are fully three-dimensional in nature. As these types of flows bear the greatest resemblance to actual particle-laden flows encountered in industry, they merit the most further study. We must study these flows more to identify where preferential concentration is occurring and to what degree it affects the statistical features of the flow.

3.3. Wall-bounded Flows

The structure of simple wall-bounded flows, including external boundary layers, channel flows and pipe flows, has been well characterized by detailed single phase experiments and numerical simulations. Much of the single phase research has been summarized in a review article by Robinson (1991). It is now generally agreed that the near wall region of the boundary layer (below y^+ of about 50) is dominated by intense longitudinal vortices which are responsible for the majority of the turbulence production. These vortices also are responsible for the long streaks of low velocity fluid which form in boundary layers as described by Kline *et al.* (1967) and many subsequent works. The longitudinal vortices trail behind arch-shaped vortices which form in the logarithmic region of the boundary layer. The outer layers of the boundary layer contain much larger arch-shaped vortices which produce relatively weak velocity fluctuations.

This section of the paper will focus on the near wall region of the wall bounded flows because there has been little work on preferential concentration in the outer region of the boundary layer.

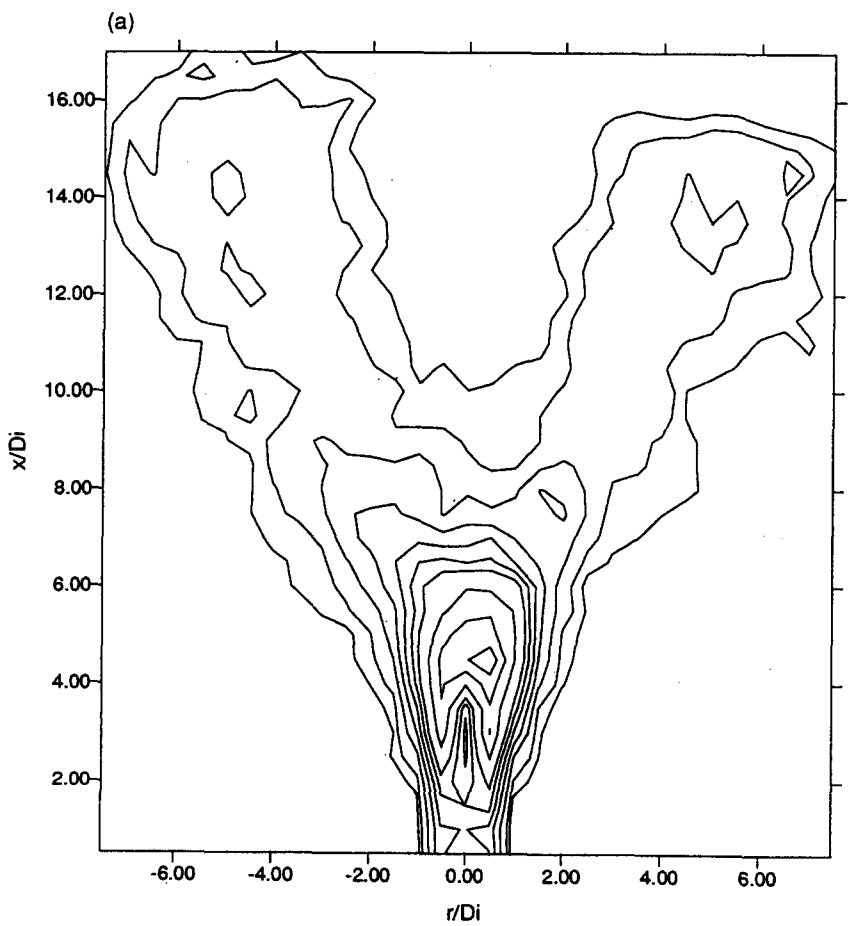

Figure 11(a). *Caption overleaf.*

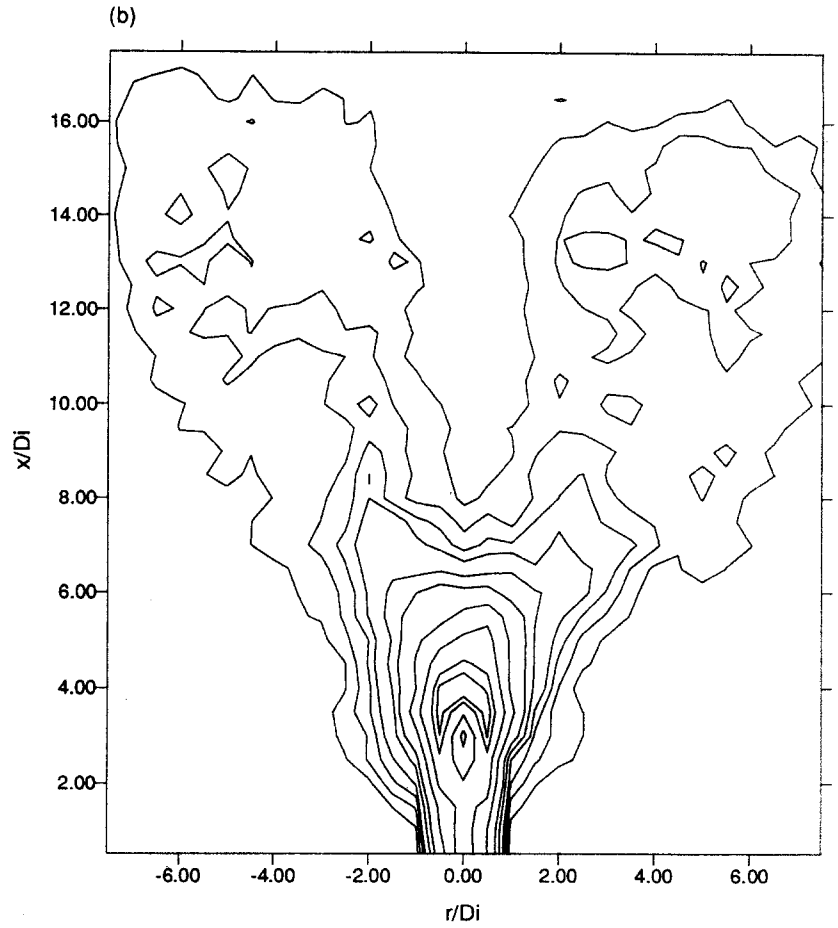

Figure 11(b)

Figure 11. Particle number density maps for a co-flowing swirling jet. Maps obtained by averaging 25 photographs of single laser pulses. (a) Unforced flow, (b) forced at 50 Hz, phase-averaged. Wicker & Eaton (1994).

Studies done near the centerline in fully developed pipe and channel flows are discussed in the section on homogeneous flows. Scaling of the flow in the near wall region is generally done in terms of the so-called wall or viscous scales. The velocity scale u^* is $\sqrt{(\tau_w/\rho)}$, the length scale is $l^* = u^*/\nu$ where ν is the kinematic viscosity, and the time scale is ν/u^{*2}. The peak levels of turbulent kinetic energy and shear stress are found at y^+ (y/l^*) near 10. The longitudinal vortices have diameters around $25l^*$ and the spacing between the streaks is around $100l^*$.

As we will see below there has been very little work done in our target parameter space: fine particles in gas flow. This is not because of lack of interest or importance of the topic but more because of experimental difficulties in observing preferential concentration at the small scales near the wall. A typical experiment might be fully developed flow of air in a 10 cm dia pipe with an average velocity of 10 m/s. For this situation, l^* is approx. 31 μm and the time scale is about 62 μs. A typical longitudinal vortex would be around 0.8 mm in dia and the streak spacing would be 3 mm. Solid particles or liquid droplets with diameters on the order of 10 μm would have time constants in the range where we might expect to find preferential concentration. However, this would be very difficult to observe experimentally because of the small scale of the structures and interference of the wall with optical visualization techniques. While the preferential concentration is difficult to observe directly it may have important effects on the flow or reaction rates which would have macroscopically observable effects.

Several studies have examined the interaction of particles with near wall vortex structures in water flows. In most of these flows the Stokes number of the particles is small because flow speeds

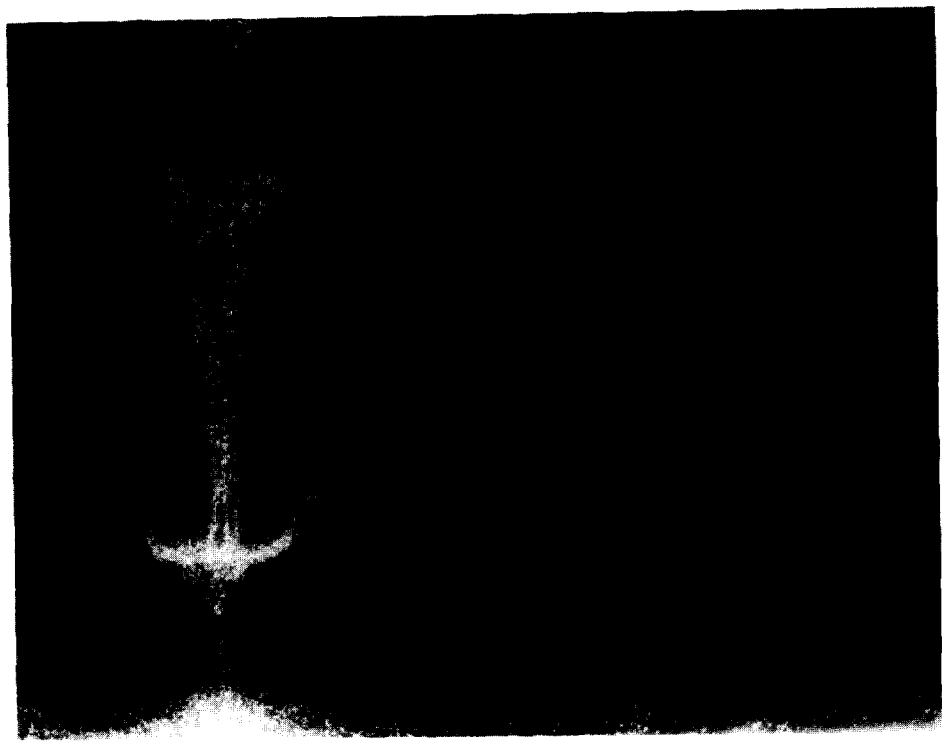

Figure 12. Visualization of smoke and particles in impinging jet. Longmire & Anderson (1993).

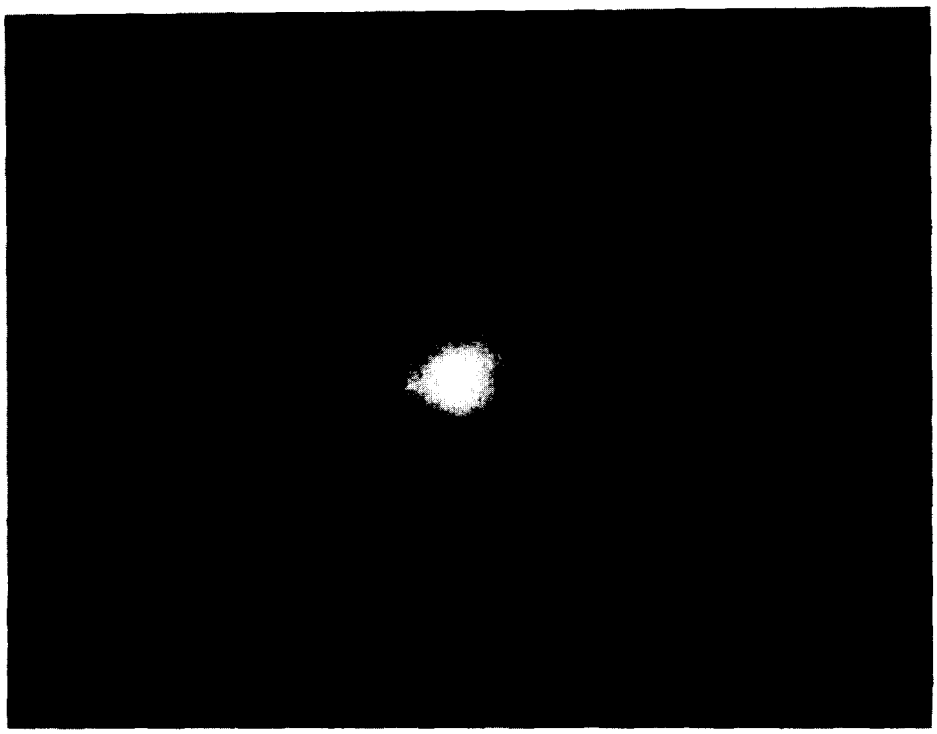

Figure 13. View of particle-laden impinging jet from figure 12 with laser sheet normal to jet flow. Photograph is taken through glass impingement plate with a laser sheet 0.6 mm off surface. Longmire & Anderson (1993).

are low and the particle densities are not much different than the water density. Also, in many cases the particle diameters are of the same order or even larger than the dominant near-wall eddies (see Sumer & Deigaard, 1981 and references therein). The primary mechanism for preferential concentration we have been discussing so far, namely centrifuging of particles out of vortices is not possible. Nevertheless, particles have been observed to collect in the low speed streaks which are certainly a coherent feature of the turbulence field. Dyer & Soulsby (1988) reviewed work on sand transport along the continental shelf. They and others found that high shear stress events in the flow over a sand bed are correlated with "... swirls of grains that can be lifted several tens of centimeters above the bed." From this description, we may surmise that the particle concentration is correlated with the vortex structure producing turbulent bursting. This mechanism is clearly different than the one we have been discussing.

In a study somewhat closer to those discussed in the rest of this paper, Rashidi *et al.* (1990) studied an open channel flow of water carrying a light loading of polystyrene particles with diameters ranging from 0.7 to 16 viscous lengths. Particles collected in the low-speed streaks and then were ejected during the bursting event except for the smallest particles which remained near the wall. In another experiment, glass particles around 0.5 viscous lengths in diameter were not ejected and had little effect on the flow. In this case the preferential concentration mechanism is the sweeping of negatively buoyant particles near the wall into the low-speed streaks by longitudinal vortices. Particles which remain suspended by larger scale turbulence away from the wall are apparently not preferentially concentrated. Direct numerical simulations were performed for similar particle parameters by Pedinotti *et al.* (1992) although the flow Reynolds number was somewhat lower. It was necessary to treat the particles as points and neglect their effect on the fluid flow. The largest particles, having time constants normalized by the viscous scales greater than 1 were found to accumulate in the low speed streaks while lighter particles remained more uniformly distributed. The strongest accumulation was seen for an intermediate time constant of $2.78t^*$. Estimating that the longitudinal vortices which cause the streaks have a typical radius of 20 viscous lengths and a typical velocity approximately equal to the friction velocity we can estimate a time scale corresponding to the vortex analysis in section 2 of around 20 viscous units. Thus, the Stokes number for the maximally concentrated particles is around 0.14, in the same range as studies in other types of flows. Unfortunately, the number of particles tracked were too small to get pictures of the instantaneous concentration field around vortices in the flow. One caution on the use of the simulations published to date is that the particles are treated as points even though their actual diameters are comparable to the radii of typical vortices.

Young & Hanratty (1991a) discussed still another effect of turbulence on the particle concentration field. They examined a vertical pipe flow of water carrying a dilute suspension of 100 μm dia glass or steel spheres. The time constants of the particles ranged from 0.5 to 18 viscous time scales but the mean relative velocity between the particles and the fluid ranged up to 1.77 times the friction velocity. The concentration of particles was so low that they could not observe preferential concentration. However, they did find evidence of turbophoresis, that is the tendency of a particle to move towards a region of lower turbulence in inhomogeneous flows (see Reeks 1983). This effect would be expected to cause variations in the mean concentration distribution. In a second paper Young & Hanratty (1991b) described necklaces of particles aligned in the streamwise direction and moving slowly along the wall of the pipe. The average spacing between the necklaces was approx. 100 wall units suggesting that the necklaces were formed by the same mechanism that forms the low-speed streaks.

Because of the experimental difficulties in examining the near-wall regions in laboratory gas flows, most observations of preferential concentration have been made using direct numerical simulations. Brooke *et al.* (1992) simulated fully developed channel flow carrying particles with the parameters selected to represent fine aerosol particles in a laboratory scale air flow. This work followed previous direct numerical simulation work by McLaughlin (1989) and an approximate simulation by Kallio & Reeks (1989) that found particles accumulating deep in the sublayer. Brooke *et al.* found the same accumulation using a higher resolution simulation and concluded that the accumulation was due to turbophoresis. They selected for detailed study particles which achieved wall normal velocities sufficient to actually impact the wall. Conditional averaging of both the particle paths and the velocity field during the particle's acceleration toward the wall indicated

that the particles were flung out of longitudinal vortices and impacted the wall. The longitudinal vortices typically had a diameter of 25 viscous lengths and a vorticity of 0.3. Using these to form a time scale as in section 2, we get Stokes numbers ranging from 0.9 to 3. Brooke *et al.* (1992) also saw a weak tendency for the largest particles that were trapped near the wall to accumulate in the low speed streaks.

In an as yet unpublished manuscript, Brooke *et al.* (1994) extended the analysis of the same simulations. They divide the particles into two classes: particles that are moving with the surrounding fluid called "entrained particles" and particles which have a significantly larger normal velocity component than the surrounding fluid called "free-flight particles". The free-flight particles are apparently those that have encountered an intense eddy and have been flung towards the wall. The free-flight particles dominate the flux of particles towards the wall inside of y^+ of 20. Turbophoresis has a smaller influence on the concentration distribution than was previously believed. An analysis of the particles that actually strike the wall shows that the greatest fractions begin their free flight around y^+ of 9. This height corresponds to the location of intense longitudinal vortices where relative motion between particles and fluid is likely to be greatest. The build up of particle concentration near the wall is thus seen as a preferential concentration effect which changes the mean rather than the instantaneous concentration distribution. Brooke *et al.* (1994) also showed probability distributions of the fluid velocities seen by particles at y^+ of 10. The distributions were narrower than the corresponding Eulerian distributions. They interpreted this as an indication that particles are "centrifuged away from turbulence-producing vortices". This is the first definitive evidence of preferential concentration in the near wall region.

Rouson & Eaton (1994) are also studying fully developed channel flow with direct numerical simulation. The Reynolds number is 1850 based on the channel half width and the centerline velocity. The Stokes number non-dimensionalized by wall variables is approx. 4.5. The difference between this calculation and the previous work of Brooke *et al.* (1992) is that a very large number of particles (approx. 370,000) are tracked allowing the instantaneous concentration field to be determined. Figure 14 shows the positions of all the particles in a thin sheet parallel to the wall centered at $y^+ = 3$. The particles are collected into the low speed streaks. Of more relevance to the present discussion is figure 15 which shows the particle positions for a plane normal to the wall. Here we can see the classic signature of preferential concentration: nearly circular voids each surrounded by a halo of particles. More analysis of these data is needed to understand the correlations between fluid structure and the particle concentration field.

Summarizing, we see that the picture of preferential concentration is far less complete in wall-bounded flows than it is in either free shear flows or the homogeneous flows to be discussed

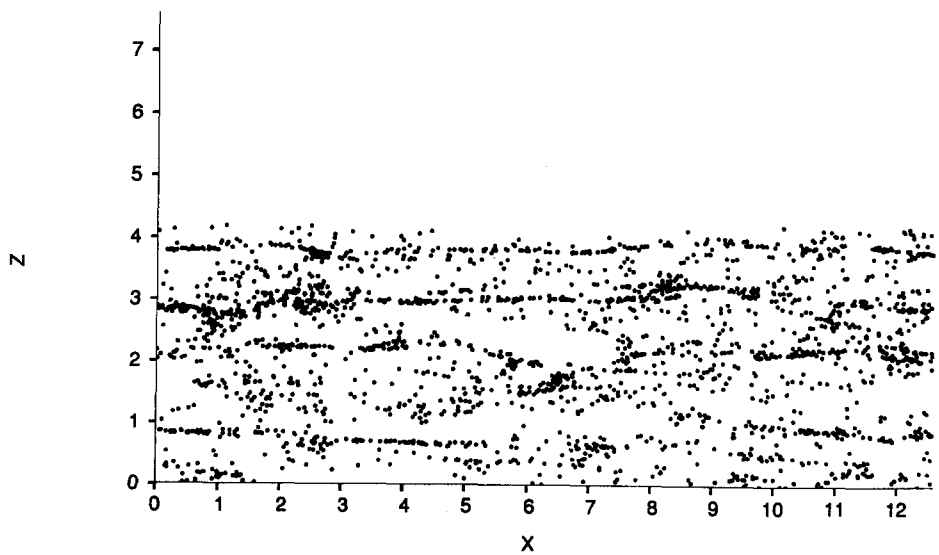

Figure 14. Instantaneous particle locations from direct numerical simulation of particle-laden channel flow. Locations are shown for particles found in the sheet parallel to the wall at $y^+ = 3$. Particles in this region are found to cluster into streaks spaced approx. 100 wall units apart. Rouson & Eaton (1994).

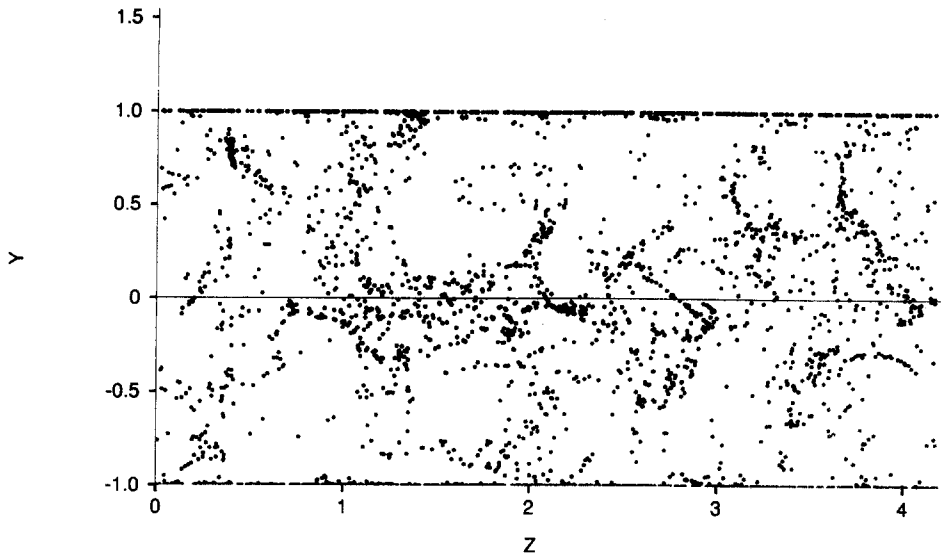

Figure 15. Instantaneous particle locations from direct numerical simulation of particle-laden channel flow. Locations are shown for particles found in the thin sheet normal to mean flow direction. Rouson & Eaton (1994).

next. Trapping of particles near the wall is a common feature of many of the flows and the collection of these near-wall particles into the low-speed streaks is well established. However, only very recently has evidence become available showing that particles are centrifuged away from the cores of the dominant longitudinal vortices. It seems important to determine just how strong this mechanism may be. With the mean concentration near the wall already being quite high, further local accumulation into regions of high strain and low vorticity may create very high local particle concentration.

3.4. Homogeneous Flows

Homogeneous turbulence has been used frequently for fundamental studies of turbulence because of its analytical simplicity. Homogeneity implies that there are no boundaries in the flow and no spatial variations in the statistical properties of the turbulence. Experimentally this has been approximated by grid turbulence, but many believe that homogeneous turbulence studies are directly relevant to many real turbulent flows including the centerline region of pipe and channel flows and freestream turbulence in complex flow geometries. Some of the earliest experiments and numerical simulations to address particle interaction with turbulence were done in homogeneous turbulence including the wind tunnel experiments of Snyder & Lumley (1971) and Wells & Stock (1983) and the numerical simulations of Riley & Patterson (1974). The main point of these works was to study turbulent diffusion of particles and to measure Lagrangian velocity correlations. None of them examined the instantaneous particle concentration field nor did they attempt to correlate the particle paths to specific turbulent structures. There have been many other analytical and numerical studies of particles moving in homogeneous turbulence. The great majority of these have examined only statistical quantities while the few reviewed here have addressed organization of the particle concentration field by the turbulent motions.

Perhaps the first notice of preferential concentration in nearly homogeneous flow was by Kada & Hanratty (1960) who examined the motion of 100 and 380 μm glass beads and 200 μm copper beads in a fully developed pipe flow of water at Reynolds numbers of 20,000 and 50,000. At the higher Reynolds number, they noted a change in behavior when the solids volume fraction was increased beyond 1.5%. Visual observations showed that the particle concentration was highly non-uniform.

Maxey & Corrsin (1986) calculated the motion of particles in a steady, two-dimensional flowfield consisting of a periodic array of eddies. The particle paths were calculated using an equation of motion which included the particle inertia, Stokes drag and gravity. The particle time constant,

the still-air settling velocity and the orientation of the gravity vector relative to the eddy array were all systematically varied. All particles having inertia were found to move away from the center of the eddies as expected. However, the lightest particles spiraled slowly outward remaining in orbit around the eddy for several cycles. Particles were found to accumulate along specific periodic paths for Stokes numbers of 0.5 or less where the Stokes number was based on the characteristic velocity and length of one of the eddies. In these studies, the dimensionless settling velocity was varied from 1/4 up to 2 with the accumulation appearing strongest at the smallest drift velocity. At the highest drift velocity, the particles still followed periodic paths but the paths were so complicated that the particles appeared to be more randomly distributed. The biggest problem with this study was that the flow was steady and in many cases it took many eddy turnover times for the particles to reach the asymptotic path. Nevertheless, the study pointed to the important possibility that particle positions may be strongly correlated to motions of turbulent eddies. The cellular flow computations were extended to non-spherical particles by Mallier & Maxey (1991) but the main emphasis of the work was on particles without inertia. Limited study was done of particles with inertia with the findings relevant to local accumulation remaining basically unchanged.

Maxey (1987) extended the earlier work by representing the turbulence as a series of randomly selected Fourier modes in which the modes are selected to form a statistically stationary, homogeneous, isotropic random field with a prescribed energy spectrum. This technique was pioneered by Kraichnan (1970) and provides a reasonable approximation of a turbulent velocity field but cannot represent the non-linear interaction between eddies of different scales. Particle paths were calculated using the same simple equation of motion. The simulations showed that the mean settling velocity of the particles was consistently between 5 and 10% higher than the still-fluid value for dimensionless settling velocities up to 1.5 and Stokes numbers ranging from 0.1 to 1. The peak settling velocity occurred around a Stokes number of 0.5. For this flow the velocity scale was chosen as the mean square velocity fluctuation and the length scale was chosen as the inverse of the wavenumber corresponding to the maximum in the energy spectrum. More important in the present context is the asymptotic analysis performed to explain the results. Separate analyses were performed for the limits of large settling velocity and small particle inertia. The latter analysis showed that the divergence of the particle velocity field is positive in regions of high vorticity and low strain rate and negative in regions of high strain rate and low vorticity. This tendency was called inertial bias of the particle trajectories. The increased averaged settling velocity was attributed to a correlation between the turbulent velocity fluctuations and the regions of high strain or low vorticity.

Fung & Perkins (1989) also represented turbulence as random Fourier modes but split the wavenumber range into small and large scales in order to represent advection of the small scales by the large-scale motions. Their main results were dispersion statistics for a range of Stokes numbers and were not relevant to the present review. However, they noted Maxey's findings of particles concentrating in streaming regions between eddies. They then proposed a rational way to divide the turbulence field into eddies, streaming zones and convergence zones (see discussion below) and proposed that this would be the appropriate way to quantify the concentration of particles within certain zones of true turbulence. The results from such an analysis were not presented.

Squires & Eaton (1990a, 1991) used direct numerical simulation of the Navier–Stokes equations to study low Reynolds number isotropic turbulence. Particle paths were calculated taking account of particle inertia and Stokes drag. Additional simulations reported in Squires & Eaton (1990b) addressed the effects of gravity and homogeneous shear. Two-way coupling was implemented in the simulations allowing the particles to modify the turbulence. A particular problem in studying true isotropic turbulence is that it is not statistically stationary; the turbulence velocity fluctuations decay and the length scales grow. This was avoided by applying a steady forcing to the turbulence at a low wavenumber using the scheme developed by Hunt *et al.* (1987). The turbulence then reached a stationary state with the turbulence level and power spectrum determined by the particle Stokes number and mass loading. One million particles were tracked amounting to an average of 103 particles in a cube with side length equal to the Kolmogorov scale. Simulations were performed for six different Stokes numbers ranging from 0.075 to 1.5 where the fluid time scale was formed using the longitudinal integral length scale and $(q^{2/3})^{1/2}$. Typical slices through the particle

concentration field are shown for zero mass loading and three different Stokes numbers in figure 16. The hydrodynamic field is identical in each case. The plots show a strong organization of the particles with the same major structures observable for all three particle time constants. The pattern is most distinct for the intermediate Stokes number of 0.15 where the peak concentration exceeds 25 times the mean value. Averaging over both space and time, it was found that approx. 42% of the computational cells contained no particles where a random particle distribution would leave only 2.5% of the cells empty. The inhomogeneity in the concentration field is weaker for both the lighter and heavier particles confirming the intuition developed in section 2 that preferential concentration should occur most strongly at an intermediate Stokes number near unity. Squires & Eaton (1990a) correlated the number density with both the vorticity and the second invariant of the deformation tensor, II_d. Regions of large positive II_d are regions of high vorticity while large negative II_d corresponds to high strain rate and low vorticity. There was a very strong tendency for the particles to concentrate in regions of high negative II_d and to avoid regions of high positive II_d as shown in figure 17. Squires & Eaton (1991) divided the flow field into zones as suggested by Fung & Perkins (1989) using the quantitative definitions developed by Hunt *et al.* (1988) and Wray & Hunt (1989). This technique classified the flow into eddies, convergence zones, streaming

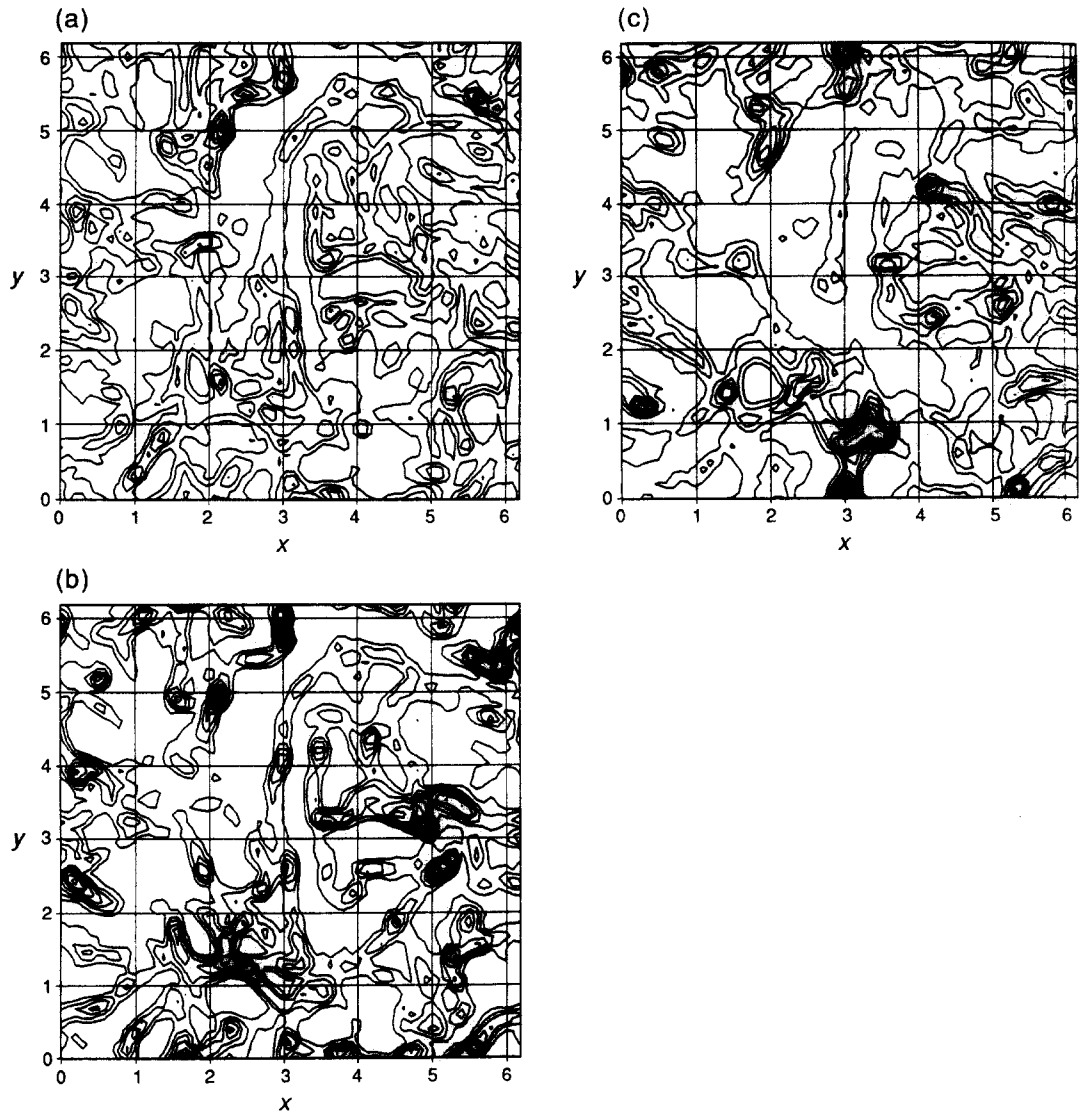

Figure 16. Particle number density maps from direct numerical simulation of homogeneous, isotropic turbulence. (a) St = 0.075, (b) St = 0.15, (c) St = 0.52. Squires & Eaton (1991).

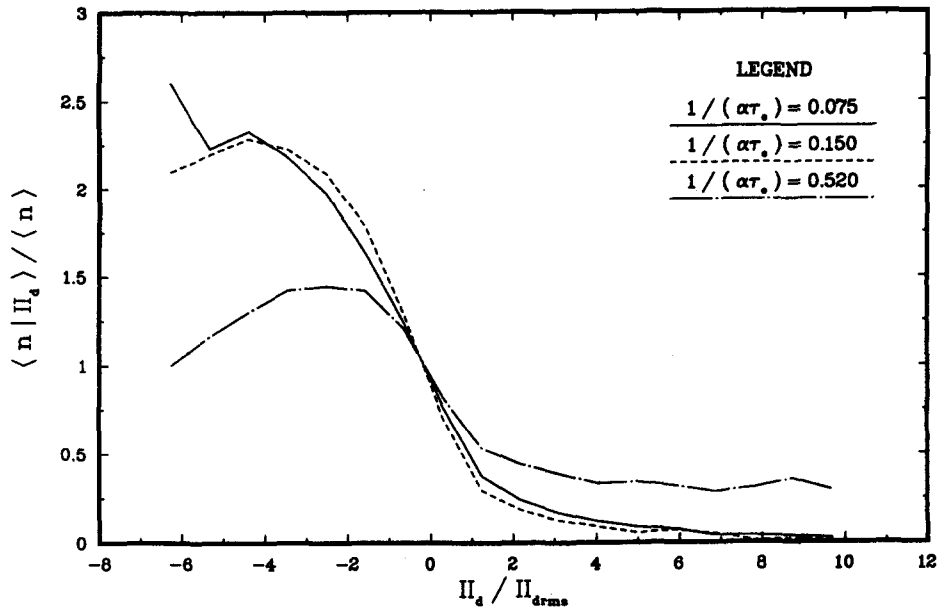

Figure 17. Conditional number density given the second invariant of deformation tensor for Stokes numbers equal to 0.075, 0.15 and 0.52. Taken from the direct numerical simulations of homogeneous, isotropic turbulence by Squires & Eaton (1990a).

zones and rotational zones, the latter being a shear layer which was not rolled up into an eddy. This technique classified approx. 53% of the domain leaving slightly less than half of the volume unclassified. A plot of the average number density in each zone as a function of particle time constant is shown in figure 18. The average concentration in convergence zones was found to be over two times the mean while the concentration in eddies was less than one quarter of the mean giving a nine to one difference in the average concentration for the two zones. Rotational and streaming zones carried intermediate concentrations.

Wang & Maxey (1993) performed similar direct numerical simulations of isotropic turbulence to examine particle settling in more realistic turbulence than Maxey's earlier work. A forcing scheme developed by Eswaran & Pope (1988) was used to maintain stationarity. As with Squires & Eaton, the low wavenumber part of the energy spectrum was distorted by the forcing but they showed that the turbulence at higher wavenumbers agreed well with previous experimental and

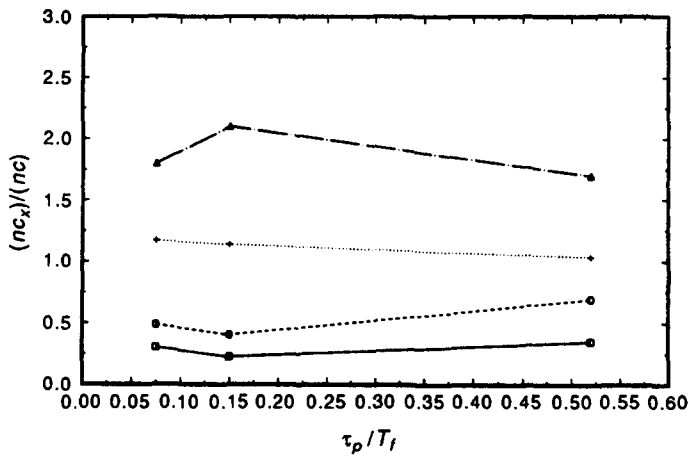

Figure 18. Zone averaged particle number density: ——, eddy; – – –, rotational; –·–·–, convergence; · · · · ·, stream. From direct numerical simulations of Squires & Eaton (1991).

analytical work. They pointed out a critical difference between free shear flows where the strongest velocity and vorticity fluctuations occur on the same large scale and homogeneous flow where the velocity fluctuations are dominated by the large scales but the intense vorticity fluctuations occur in tube like structures at dissipation range scales. A large number of particles (131,072) was tracked for a single case to obtain instantaneous concentration distributions. The Stokes number and still-fluid settling velocity were both set equal to 1 when normalized by Kolmogorov scales. Five slices through the concentration field are shown along with plots of the scalar vorticity in figure 19. The plots look quite similar to Squires & Eaton's and a strong correlation between the regions of low concentration and high vorticity is apparent. Maximum concentrations ranged between 20 and 50 times the mean. They also observed that "regions of higher particle concentration tend to appear as long, connected patches or sheets that are aligned vertically". They found that the combination of gravity and inertial bias causes the particles to be clustered in downward moving streaming flows between vortical regions. To quantify the deviation of the particle concentration field from a statistically uniform grid they formed a new statistic:

$$D_C = \sum_{C=0}^{N_D} (P_C(C) - P^u_C(c))^2$$

where $P_C(C)$ is the probability of finding an integral number C of particles in a given cell and $P^u_C(C)$ is the equivalent probability for a random distribution of particles. Thus D_C is the mean square deviation of the particle concentration distribution from a random distribution. Figure 20 shows D_C plotted as a function of Stokes number. The peak deviation occurred for Stokes number near unity. When Squires & Eaton's Stokes numbers were renormalized by the Kolmogorov time they were found to be in rough agreement. The still-air settling velocity was also varied holding the Stokes number fixed at 1. The preferential concentration was found to be strongest at 0 settling velocity but it was still quite significant for settling velocities up to three times the Kolmogorov velocity scale.

While the simulations of Squires & Eaton, and Wang & Maxey have cast considerable light on preferential concentration in homogeneous turbulence, there is still some worry about the effect of the forcing schemes used. Generally, preferential concentration has taken place on scales shorter than the forcing scales and significantly different forcing schemes have yielded similar results. Nevertheless, experimental confirmation of these results is desirable. To date, there have been no grid turbulence experiments with sufficiently large particle concentration to observe preferential concentration. However, there have been two experiments which have examined the distributions of particle concentration near the centerline of a pipe and on the centerplane of a channel flow. These two flows offer a reasonable approximation of stationary homogeneous turbulence with the stationarity maintained by turbulent diffusion rather than artificial forcing.

Neumann & Umhauer (1991) used pulsed laser holography to measure the positions of particles near the centerline of a 50 mm dia pipe flow. The particles were either 40–50 μm glass beads or polydisperse (2–95 μm) water droplets. Unfortunately, no information was given on the turbulent flow except for the mean velocity which ranged from 2.8 to 6.8 m/s. Slices showing the position of every water droplet showed regions of high droplet concentration and other regions devoid of droplets. The distance to the nearest neighboring particle was calculated for every particle in the measurement volume. The distribution function was compared to a random distribution. The distributions deviated strongly for the glass beads indicating that preferential concentration had occurred.

Fessler *et al.* (1993) examined the particle concentration distribution on the centerplane of a vertical turbulent channel flow. Five different sets of size classified particles with Stokes numbers ranging from 0.7 to 41 were used. The Kolmogorov time scale estimated using a k–ϵ calculation of the flow was used to compute the Stokes number. The still-air settling velocity varied from 0.2 to 11.5 times the Kolmogorov velocity scale. The concentration field was obtained by digitizing photographs of particles illuminated by a laser sheet on the centerplane and identifying individual

Figure 19 (*facing page*). Particle concentration field (left-hand side) and flow scalar-vorticity field (right-hand side) at five consecutive times spaced roughly one Kolmogorov time scale (τ_k) apart. Stokes number for particles (τ_p/τ_k) = 1.0. Wang & Maxey (1993).

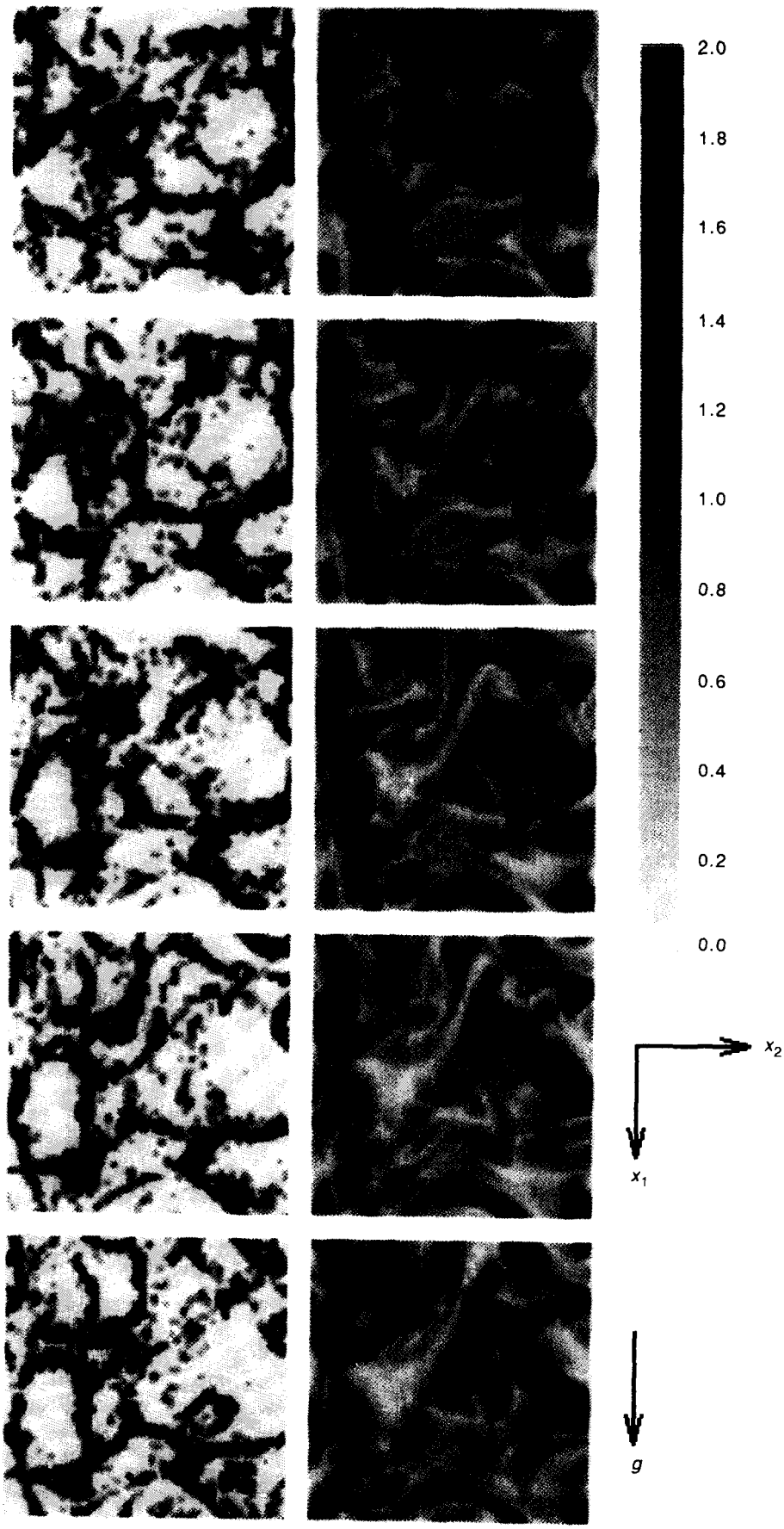

Figure 19

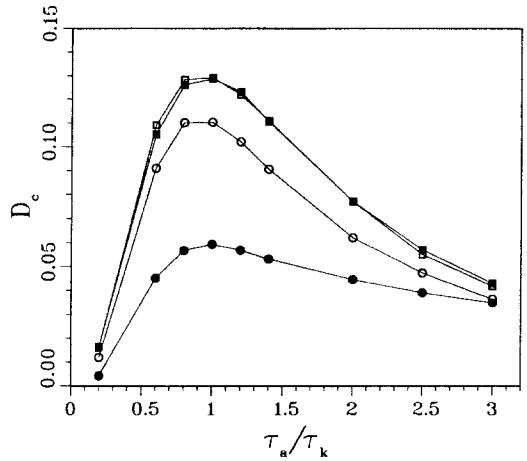

Figure 20. Temporal evolution of deviation of particle concentration distribution from randomness vs Stokes number. ●, $t/\tau_k = 6.8$; ○, $t/\tau_k = 13.6$; ■, $t/\tau_k = 20.4$; □, $t/\tau_k = 27.2$. Wang & Maxey (1993).

particles. Figure 21 shows photographs for three particle sizes. Figure 21(a) looks remarkably like the previous DNS results although there is no evidence of alignment of particle clusters along vertical paths as suggested by Wang & Maxey. Preferential concentration is also apparent for the intermediate size particles although it should be noted that the preferential concentration appears on a larger length scale. The largest particles examined appear to be randomly distributed. In order to quantify the deviation of the concentration field from a random distribution, 10–15 photographs were digitized for each particle size. Each photograph was divided into square boxes and the distribution of the number of particles per box calculated. The resulting distribution was compared to the Poisson distribution expected for a random distribution of the same mean number of particles per box. The particles with the largest Stokes number matched the Poisson distribution very closely indicating that no preferential concentration occurs. The lighter particles deviated strongly from the Poisson distribution (see figure 22) with many boxes containing either zero or a large number of particles. To capture the variation of scale seen in figure 21, the photographs were analyzed using boxes with a range of sizes. A scalar parameter, D was defined to indicate the deviation of the distribution from randomness:

$$D = (\sigma - \sigma_p)/\mu$$

where σ and σ_p are the standard deviations of the actual and random distributions and μ is the mean number of particles per box. A plot of D vs box size is shown in figure 23. The location of the peak is a function of particle size; the smallest particles are preferentially concentrated at the smallest scales while the larger particles are concentrated at larger scales. The dependence of the scale on particle size was confirmed by measurement of the power spectrum of laser light scattered from 1 mm^3 volume. The maximum preferential concentration occurs for particles around Stokes number of 1 in agreement with Wang & Maxey (1993).

Summarizing, both simulations and experiments have helped us reach a reasonably good understanding of preferential concentration in homogeneous flows. Preferential concentration appears to be important for a range of particle sizes with the peak concentrations occurring at Stokes number based on the Kolmogorov time scale close to 1. Significant preferential concentration occurs for Stokes numbers up to 10. The lower bound has not been established. This seems like an appropriate topic for further simulation. The length scale on which the preferential concentration occurs is dependent on the Stokes number. Particles around Stokes number of 1 are concentrated at length scales in the dissipation range (6–20 Kolmogorov lengths) while heavier particles can only be affected by the larger scales in the flow. Two mechanisms, centrifuging of

Figure 21 (*facing page*). Photographs of particles illuminated by X–Z laser sheet at channel centerline. (a) 28 μm Lycopodium, St = 0.7, (b) 50 μm glass, St = 8, (c) 70 μm copper, St = 41. Fessler *et al.* (1994).

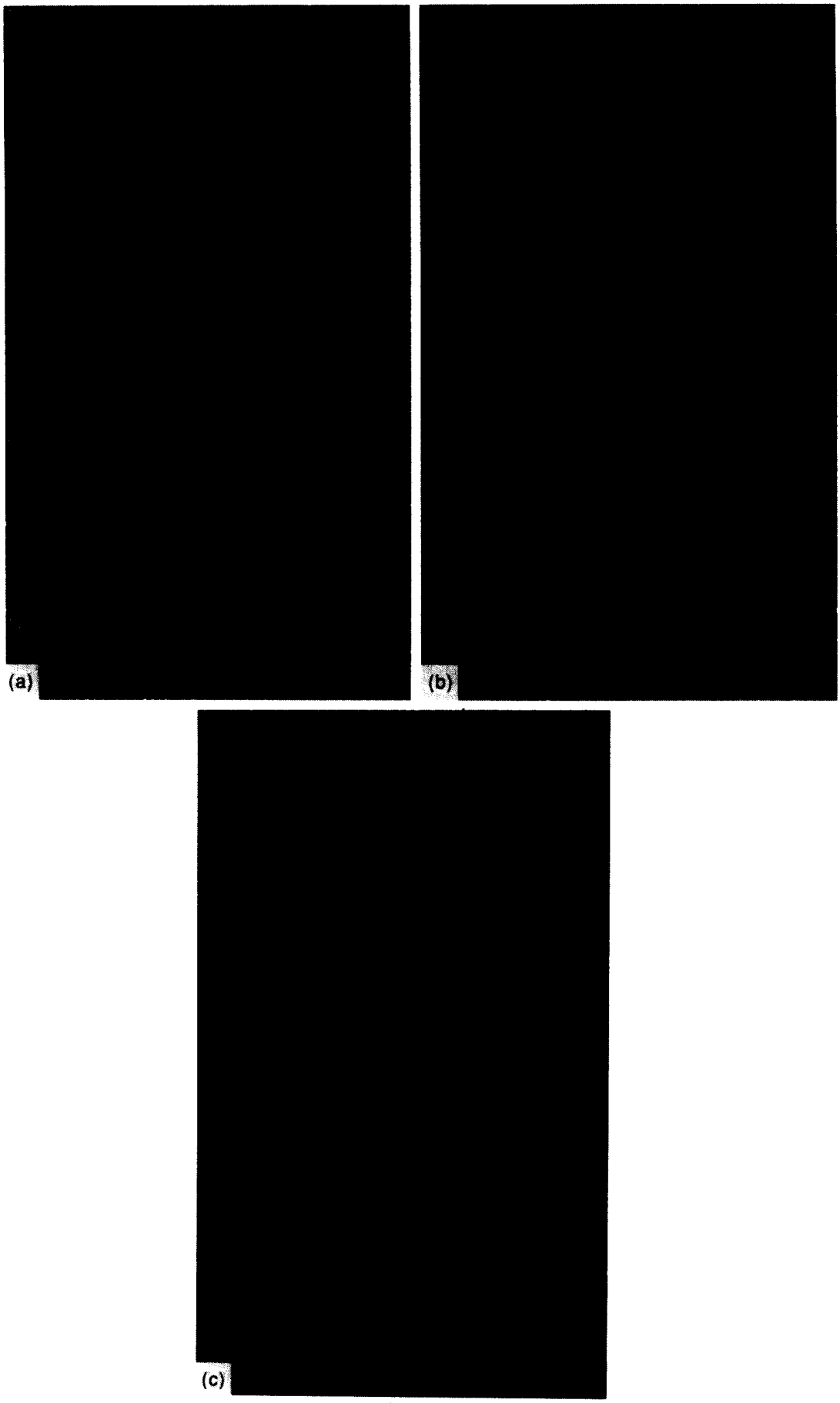

Figure 21

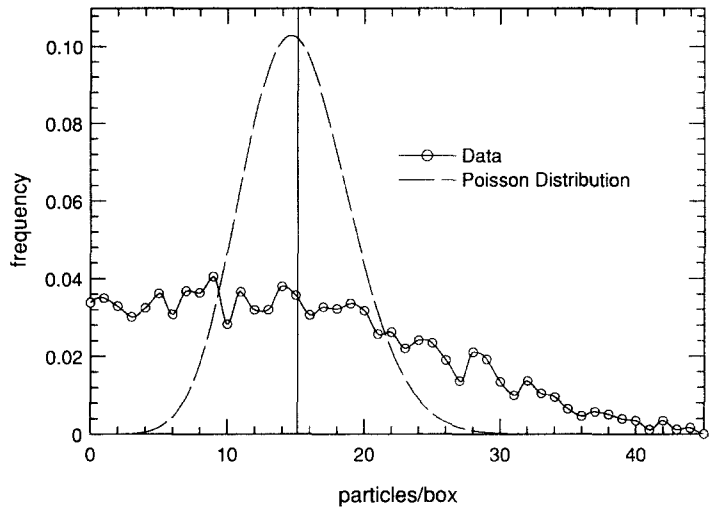

Figure 22. Distribution of particle number density for 28 μm Lycopodium particles, St = 0.7, on a 2 mm square grid. Also plotted is Poisson, or random distribution, for the same mean number of particles per box. Fessler *et al.* (1994).

particles from vortices and collection of particles in convergence zones seem to be important in causing preferential concentration.

4. THE EFFECT OF PREFERENTIAL CONCENTRATION ON TURBULENCE

Recently, there has been interest in understanding how turbulence is modified by the presence of moderate loadings of particles. Gore & Crowe (1989) and Hetsroni (1989) have published brief reviews on this subject. Their basic conclusions were similar; fine particles attenuate turbulence while large particles increase it. They differed on the appropriate definition of large and small. Gore & Crowe found that the particle diameter normalized by a turbulence length scale was the parameter which determined if the turbulence would be increased or decreased. Hetsroni (1989) concluded that the particle Reynolds number is the governing parameter. In this paper we have been mainly interested in fine particles that would be expected to cause attenuation of turbulence. It has been found that dispersed particles can cause significant reductions in the turbulence levels for mass loading ratios of 10% or greater. For example, Kulick *et al.* (1993) observed reductions as large as 50% in a fully developed channel flow with a mass loading of 40%. As we have seen,

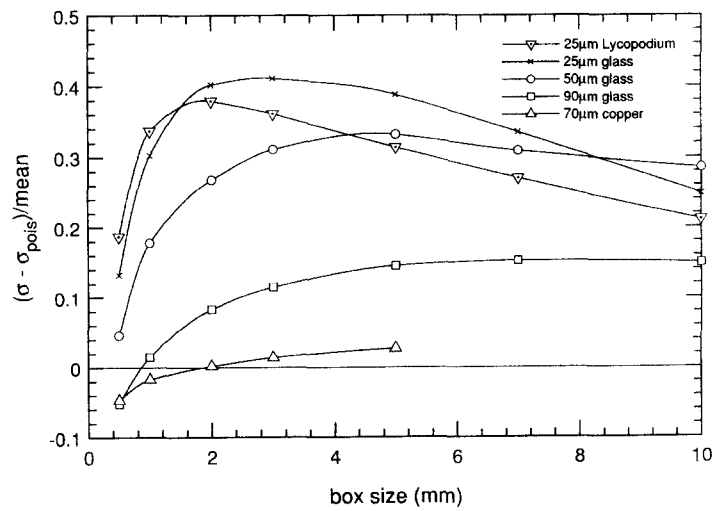

Figure 23. Deviation of particle concentration distribution from randomness, D, vs box size for five particle sizes. Fessler *et al.* (1994).

preferential concentration can create strong correlations between the particle concentration field and the fluid velocity field. One might guess then that preferential concentration would have a significant effect on the turbulence attenuation. However, there has been little research to date to address this issue. This section reviews the previous work and offers a simple analysis which may lead to some insight.

An obvious place to start this discussion is the transport equation for the turbulence kinetic energy. Kulick *et al.* (1993) derived the equation assuming that the particles are small relative to the smallest eddies in the flow, that the particles have a linear (Stokes) drag law, and that the flow is homogeneous:

$$\frac{\mathrm{d}k}{\mathrm{d}t} = \frac{\mathrm{d}k}{\mathrm{d}t}\bigg|_{\text{s.-p.}} - \frac{\bar{C}}{\rho\tau_\mathrm{p}}(\overline{u_i u_i} - \overline{u_i v_i}) - \frac{1}{\rho\tau_\mathrm{p}}(\overline{c u_i u_i} - \overline{c u_i v_i}) - \frac{1}{\rho\tau_\mathrm{p}}(\bar{U}_i - \bar{V}_i)\overline{c u_i}. \qquad [1]$$

where k is the turbulent kinetic energy, c is the fluctuating particle concentration, u_i are fluid velocity components, v_i are particle velocity components and ρ is the fluid density. The first term on the right-hand side represents all the terms found on the right-hand side of the single phase kinetic energy transport equation. The important feature of this equation in the present context is that correlations between the particle concentration and the fluid velocity appear explicitly. These terms are normally neglected in models of particle-laden flows probably because the modelers have no way to estimate their magnitude. However, it seems critical to investigate the importance of these terms before the available models can be trusted for practical applications.

There has been extensive study of preferential concentration in the plane mixing layer but no research has been reported on the effect of the preferential concentration on the turbulence. Yang *et al.* (1990) performed a linear stability analysis for a mixing layer laden with dense particles. The results showed that the growth rate of instability waves was reduced although the most amplified wavelength is approximately the same as a single phase layer. This study cast some light on turbulence modification but did not explicitly address the effect of preferential concentration.

To analyze the effect of preferential concentration on mixing layer vortices, we return to the simplified analysis of section 2 and make use of qualitative observations of preferential concentration in mixing layers and axisymmetric jets. It was found that particles are "folded" into the vortex core during the pairing process and then subsequently flung out. We will extend the analysis to calculate the torque applied to the fluid by a particle and to determine the total angular impulse applied to the fluid by the particles during the time it takes the particles to exit the vortex core. For our analysis, we assume that we have a Rankine vortex that has just formed via initial rollup or by pairing. The particles are initially uniformly distributed throughout the core and have zero velocity relative to the vortex. We further assume that the particle material density is much greater than the fluid density, that gravity can be neglected and that the particle Reynolds number is always small.

Under these assumptions, the only force experienced by the particle is the Stokes drag. We can compute the path of a particle and for Stokes numbers around 1 we find that the particle is accelerated and flung out of the vortex core as illustrated in figure 1. The Stokes drag at each point along the particle's path may be resolved into radial and tangential components. The particle applies a reaction force on the fluid and the tangential component of this force applies a torque which tends to slow the rotation of the vortex.

$$\begin{aligned} T_i(t) &= F_{t_i}(t) \cdot r_i(t) \\ &= 3\pi d_\mathrm{p}\mu[U_\mathrm{t}(r) - V_{t_i}(t)]r_i(t) \end{aligned} \qquad [2]$$

where $T_i(t)$ is the torque applied by the ith particle, r_i is the radial position of the particle, V_{t_i} is the tangential velocity of the particle and $U_\mathrm{t}(r)$ is the tangential velocity of the fluid at the radial position of the particle. The fluid velocity is assumed to be independent of time. This torque may be integrated over the time that the particle remains in the core to determine the total angular impulse applied by the particle to the fluid in the core.

$$H_i = \int_0^{t_{c_i}} 3\pi d_\mathrm{p}\mu[U_\mathrm{t}(r) - V_{t_i}(t)]r_i(t)\mathrm{d}t \qquad [3]$$

where H_i is the angular impulse and t_{c_i} is the time it takes the particle to travel from its initial position to the edge of the core. Defining h_i as:

$$h_i = \int_0^{t_{c_i}} [U_t(r) - V_{t_i}(t)] r_i(t) \mathrm{d}t \qquad [4]$$

we may write the angular impulse due to a single particle as:

$$H_i = 3\pi d_p \mu h_i \qquad [5]$$

The integral in [3] was performed numerically for particles with Stokes number equal to 1 and beginning at various initial radii. The results were nearly independent of the initial radius with an average of $h_i = 0.65 r_0^2$, where r_0 is the core radius.

The number of particles initially contained in the vortex core per unit depth is:

$$N_p = \frac{6\phi \rho_f r_0^2}{\rho_p d_p^3} \qquad [6]$$

where ϕ is the mass loading ratio. Then the total angular impulse applied to the vortex core per unit depth during the time it takes the particles to be flung out is:

$$\begin{aligned} N_p H_i &= \frac{6\phi \rho_f r_0^2}{\rho_p d_p^3} 3\pi d_p \mu h_i \\ &= \frac{18\mu}{\rho_p d_p^2} \phi \rho_f \pi r_0^2 h_i \\ &= 0.65 \pi r_0^4 \phi \rho_f / \tau_p \end{aligned} \qquad [7]$$

The initial angular momentum of the vortex core per unit depth is:

$$\frac{\pi}{2} \rho_f V_0 r_0^3$$

So the ratio of the angular impulse to the initial fluid angular momentum is:

$$\frac{1.3\pi r_0^4 \phi \rho_f / \tau_p}{\rho_f V_0 r_0^3} = \frac{1.3\phi r_0}{\tau_p V_0} = \frac{1.3\phi}{\mathrm{St}} \qquad [8]$$

To arrive at the constant of 0.65 we assumed a Stokes number of 1 so the final result shows that the fraction of the initial angular momentum taken by the particles is 1.3ϕ. For a mass loading of 20%, the simple analysis shows that the particles would slow the rotation of the core by 26% during the period when the particles are flung from the core. This analysis is oversimplified but it suggests that preferential concentration may have a very significant effect on mixing layer vortices. This would be an appropriate topic for further research.

Rashidi *et al.* (1990) observed a much different mechanism of turbulence modification in their water channel studies. As previously mentioned, they found that the polystyrene particles were strongly concentrated in the low speed streaks. The largest particles (1100 μm dia) had diameters on the same order as the dominant longitudinal vortices and caused an increase in the number of wall ejections (bursts) and a corresponding increase in the turbulence levels. The 120 μm polystyrene particles also collected in the low-speed streaks but caused a decrease in the frequency of ejections and in the turbulence intensity.

Squires & Eaton (1990a) examined turbulence attenuation in homogeneous turbulence using a direct numerical simulation technique which provided for two-way coupling between the particle and fluid phase momentum equations. Mass loading ratios ranging from 0 up to 1.0 and Kolmogorov Stokes numbers ranging from 0.6 to 6.5 were investigated. In the forced, homogeneous simulations the energy input from the forcing is balanced by viscous dissipation at the small scales. Adding particles adds an additional dissipation (dissipation due to particles) so the turbulence kinetic energy decreases. The ordinary viscous dissipation also decreases as the turbulence is attenuated. Reexamining the earlier simulations, Squires & Eaton (1994) found that the turbulence attenuation was strongest for the lightest particles. Preferential concentration was very strong for these light particles and relatively mild for the heaviest particles (see section 3.4).

The numerical data were used for direct evaluation of the constants used in the standard implementation of the k–ϵ model for particle laden flow (c.f. Elghobashi & Abou-Arab 1984; Berlemont *et al.* 1990). Normally it is assumed that the dissipation rate is reduced by the particles in proportion to the reduction of the kinetic energy. However, Squires & Eaton (1994) showed that the particles actually acted to increase the dissipation rate when preferential concentration was strong. They concluded that the preferential concentration acted to increase small-scale vorticity fluctuations thus increasing the dissipation rate. The term in the dissipation rate equation representing the destruction of dissipation by viscosity was also evaluated. This term was found to depend strongly on the mass loading when preferential concentration occurs. The overall conclusion that may be reached is that the turbulence is highly distorted by the presence of preferential concentration at significant mass loadings. Elghobashi & Truesdell (1993) also performed direct simulations of homogeneous turbulence with two-way coupling. They examined decaying (unforced) isotropic turbulence. Particle time constants were in the same range where Squires & Eaton (1991) and Wang & Maxey (1993) found preferential concentration to be strong. They also found that the particles increased the viscous dissipation rate but they did not attribute this increase to preferential concentration.

5. MORE EFFECTS OF PREFERENTIAL CONCENTRATION

Section 3 has presented ample evidence that preferential concentration occurs in a wide range of flow situations and over a broad range of particle parameters which encompass many practical applications. In some cases it occurs on a very large scale making gross variations in the particle concentration. In other cases, it occurs on a very fine scale, clustering particles into small groups of very high concentration. We must now ask how this information might be used? What are the possible impacts of preferential concentration in technological and natural flows?

Perhaps the most obvious application of interest is in the combustion of particulate fuels like pulverized coal. Typical small-scale burners are likely to have preferential concentration at the largest scales of motion. On the other hand, preferential concentration would probably only occur at dissipation range scales in the large burners used in utility boilers. In either case, the concentration distribution is far from uniform. Models for coal combustion generally assume that the particles are homogeneously distributed over some region. However, an individual burning coal particle can only know about its local environment. A particle which is collected into a high strain region of the flow may burn in a very fuel-rich environment even though the time-averaged stoichiometry may be quite lean. Preferential concentration may cause considerable problems in scaling a burner from laboratory to prototype scale. The combustion characteristics may be significantly different if preferential concentration occurs at one scale but not at the other.

Another area of interest in the combustion arena should be in flammability limits of dilute suspensions of combustible particulates. A detonation wave can propagate through the suspension if the fuel concentration is high enough that the heat transfer away from the flame is balanced by the heat gain from the reaction. Preferential concentration may allow a flame to propagate through a suspension with a mean concentration below the normal flammability limit. Such an effect may be responsible for variability in measured flammability limits.

Preferential concentration can also greatly affect the evaporation and combustion of liquid droplets. For example, the model of Bellan & Harstad (1988) shows that the evaporation characteristics of dense clusters of droplets are significantly different than those for dilute clusters. In particular, the size of the cluster and interactions with gas phase turbulence govern the evaporation rate of dense clusters while these factors have no effect on the evaporation rate for dilute clusters. Fichot *et al.* (1993) modeled the effects of a vortex on the evaporation and combustion of a cluster of droplets. The droplets in the model are centrifuged out of the vortex core into a thin ring of high droplet concentration, leaving the core filled with fuel vapor. Although combustion initiates inside the cluster, the ring of liquid droplets quickly cools the vortex core to the point where further combustion is impossible. After this point, combustion only occurs on the outside of the droplet clusters.

The extensive analytical work of Maxey and coworkers has shown that preferential concentration causes significant increases in the average settling rate of particles suspended in a turbulent

flow. Preferential concentration may also affect agglomeration of particles. In many systems, fine particles are agglomerated to enhance settling. A typical example is in electrostatic precipitators where fluctuating electric fields have been used to promote agglomeration of fly ash particles. Turbulence of the appropriate scale might be very effective in creating dense clusters of particles which would then be more likely to agglomerate. Enhanced agglomeration of particulates due to preferential concentration is also thought to be important in the formation of planets from protoplanetary nebula (Cuzzi 1994).

In all of the applications mentioned above, preferential concentration may play a significant role in determining the overall system behavior even if it occurs on a very small scale. It seems apparent that the models designed to represent particle-laden flows must be able to determine whether preferential concentration will occur and account for it when it does occur. Present computational models represent only the time-averaged statistical properties of the flow and have no way to resolve the instantaneous concentration field. This deficiency is most apparent in flows like the axisymmetric jet and plane mixing layer where flow visualization has shown particles grouped into large-scale clusters yet models show only a mean concentration profile. It may be possible to parameterize the effects of preferential concentration on the time averaged properties of the flow and represent these effects by further approximate models. However, such an approach would require a large amount of empiricism and there are not sufficient experiments to support such an approach.

In order to simulate preferential concentration directly, a model must provide the instantaneous fluid velocity field. Given this, preferential concentration can be estimated using a Lagrangian particle tracking scheme or possibly with a two-fluid model. There are presently three techniques which are used to supply the instantaneous velocity field. The first is direct numerical simulation (DNS) in which the three dimensional, time-dependent Navier–Stokes equations are computed with sufficient resolution to capture all the scales of motion in the flow. This approach has been used successfully in several of the studies cited above. However, DNS is limited to very simple flows at low Reynolds number because the required resolution leads to computationally intensive simulations. Its use is likely to be restricted to basic studies of particle-laden flows for development of approximate models. A second approach that has been taken is the use of Lagrangian vorticity tracking codes in which small blobs of vortical fluid are tracked through the flow. This technique is likely to be important for cases in which preferential concentration occurs on a large scale. Chein & Chung (1988) have been successful in representing particle-laden free shear layers using this approach. This technique, however, becomes considerably more complex when the flow is three-dimensional and when solid surfaces are present. The third method is large-eddy simulation in which the largest scales of motion are computed directly while the smaller (sub-grid) scales are modeled (see review of Rogallo & Moin 1984). This technique has been tested for many single-phase flows and recently developed advanced sub-grid-scale models have provided excellent results in simple flows. The first tests of large eddy simulation in particle-laden flows are just now under way (Deutsch & Simonin 1991; Aggarwal & Uthuppan 1993) but to date none have incorporated a sub-grid-scale model. Large eddy simulation seems like an ideal approach for flows like the mixing layer where the preferential concentration is caused by the largest scales of motion. It may not be effective, however, in flows where the concentration occurs at smaller scale as in the homogeneous flows described above. High Reynolds number flows will be especially troublesome as the range of scales is very large. In these cases it may be necessary to incorporate the effects of preferential concentration into the sub-grid-scale model.

A large number of research studies have now established that preferential concentration occurs in many flows. However, except in two narrow fields, combustion of droplet clusters and settling of aerosol particles there has been very little done to understand its effects on the overall system behavior. Also, little effort has been devoted to developing models that account for preferential concentration. It seems appropriate at this time to study in detail how the local accumulations of particles affect such things as turbulence modification, combustion, agglomeration, drying or solidification of particles. We have argued above that preferential concentration may have significant effects in such areas as pollutant formation, electrostatic precipitator collection efficiency and product yield in particulate processing. If this turns out to be true, it will be crucial to develop appropriate models.

6. SUMMARY

It is obvious from the review of section 3 that there has been much recent research into the phenomenon we have called preferential concentration of particles by turbulence. This research has firmly established that preferential concentration occurs over a wide range of flowfields and over a range of particle sizes which incorporate many practical applications. The same basic mechanisms are operable in most flows, namely centrifuging of particles away from vortices and concentration of particles in regions of high strain and low vorticity. Preferential concentration is strongest for Stokes numbers near 1 where the fluid time scale is appropriate for the vortex motions which actually cause the preferential concentration. In most turbulent flows, however, there are fairly intense vortical structures with a range of scales. Particles may be concentrated on different scales depending on the particle size so a unique fluid time scale cannot be defined for a given flow.

The most extensive study of preferential concentration has been in free shear flows where the emphasis has been on the interaction of particles with large-scale, two-dimensional vortices. Particles have been found to collect in a halo around the vortices with the particle cloud then folded back into the shear layer during vortex pairing. The details of the interaction are dependent on the initial particle position, the Stokes number and the orientation of a body force. Effective control of particle dispersion and clustering has been demonstrated in mixing layers and jets. Studies in complex free shear flows have shown that preferential concentration is not restricted to simple geometries. Useful models have been developed to predict particle motion in simple free shear flows but the extension of these models to complex flows is not straightforward. There has been no study of preferential concentration by intermediate scale motions such as the braid vortices in the mixing layer. Our expectation is that these vortices may produce concentration inhomogeneities in shear flows where the particles are too small to be concentrated by the large scale vortices.

In wall-bounded flows there has been much less research probably because of the difficulty of observing preferential concentration in the complex three-dimensional turbulence which occurs at very small scale near the wall. A local increase in the mean concentration adjacent to the wall is produced by vortices which fling particles into the viscous sublayer where they become trapped. Particles are swept into the low speed streaks and in some flows ejected from the wall by bursting motions. Further research is needed to determine if the regions of locally high concentration are formed by the intense longitudinal vortices which are present near the wall or the large scale but less intense arch-shaped vortices found farther from the wall.

Particle motion in homogeneous turbulence has been studied using direct numerical simulation and experiment. The simulations which are restricted to low Reynolds numbers have shown that particles are most strongly concentrated when the Stokes number based on Kolmogorov scales is near 1. Experiment has supported this conclusion but has also shown that the scale of the preferential concentration is dependent on the particle time constant. When the particle loading is sufficiently large, the concentrations of particles may distort the turbulence increasing the viscous dissipation of turbulence and thereby reducing the turbulent kinetic energy.

Models capable of representing preferential concentration are presently at a very early stage of development. Large eddy simulation seems to hold the most promise of being capable of capturing preferential concentration in many different types of flows. However, considerable effort is needed in order to develop appropriate sub-grid scale models which incorporate the effects of preferential concentration at the small scale. To date, there has been little recognition of the effect of preferential concentration in practical applications. We believe that as this phenomenon becomes more well known, its effects will be recognized as significant in many applications.

Acknowledgements—We thank Dr Hetsroni for the invitation and encouragement to submit this paper. We have benefited greatly from discussions with our colleagues, Damian Rouson and Ryan Wicker, and the comments of Professors Ellen Longmire and Kyle Squires. Professor Tim Troutt, Dr L. P. Wang and Mr Steve Anderson generously supplied us with original figures. Our own research in particle-laden flows has been generously supported by the National Science Foundation (CTS 9005 998) and the Electric Power Research Institute (RP8005-2).

REFERENCES

AGGARWAL, S. K. & UTHUPPAN, J. 1993 Dispersion enhancement in the near region of an externally forced jet. *Bull. Am. Phys. Soc.* **38,** 2279.

BACHALO, W. D., BACHALO, E. J., HANSCOM, J. & SANKAR, S. V. 1993 An investigation of spray interaction with large-scale eddies. AIAA 93-0696.

BELLAN, J. & HARSTAD, K. 1988 Turbulence effects during evaporation of drops in clusters. *Int. J. Heat Mass Transfer* **31,** 1655–1668.

BERLEMONT, A., DESJONQUERES, P. & GOUSEBET, G. 1990 Particle-Lagrangian simulation in turbulent flows. *Int. J. Multiphase Flow* **16,** 19–34.

BERNAL, L. P. & ROSHKO, A. 1986 Streamwise vortex structures in plane mixing layers. *J. Fluid Mech.* **170,** 499–525.

BROOKE, J. W., HANRATTY, T. J. & MCLAUGHLIN, J. B. 1994 Free-flight mixing and deposition of aerosols. Manuscript submitted for publication.

BROOKE, J. W., KONTOMARIS, K., HANRATTY, T. J. & MCLAUGHLIN, J. B. 1992 Turbulent deposition and trapping of aerosols at a wall. *Phys. Fluids A* **4,** 825–834.

BROWN, G. L. & ROSHKO, A. 1974 On the density effects and large structure in turbulent mixing layers. *J. Fluid Mech.* **64,** 693–704.

CHEIN, R. & CHUNG, J. N. 1987 Effects of vortex pairing on particle dispersion in turbulent shear flows. *Int. J. Multiphase Flow* **13,** 785–802.

CHEIN, R. & CHUNG, J. N. 1988 Particle dynamics in a gas-particle flow over normal and inclined plates. *Chem. Engng Sci.* **43,** 1621–1636.

CHUNG, J. N. & TROUTT, T. R. 1988 Simulation of particle dispersion in an axisymmetric jet. *J. Fluid Mech.* **186,** 199–222.

CROWE, C. T., CHUNG, J. N. & TROUTT, T. R. 1988 Particle mixing in free shear flows. *Prog. Energy Combust. Sci.* **14,** 171–194.

CROWE, C. T., CHUNG, J. N. & TROUTT, T. R. 1993 Particle dispersion by organized turbulent structures. In *Particulate Two-phase Flows* (Edited by ROCO, M. C.), Chap. 18. Butterworth–Heinemann, New York.

CUZZI, J. 1994 Personal communication.

DEUTSCH, E. & SIMONIN, O. 1991 Large eddy simulation applied to the modelling of particulate transport coefficients in turbulent two-phase flows. In *Proc. 8th Symp. Turbulent Shear Flows*, Munich, pp. 10-1-1–10-1-6.

DYER, K. R. & SOULSBY, R. L. 1988 Sand transport on the continental shelf. *Ann. Rev. Fluid Mech.* **20,** 295–324.

ELGHOBASHI, S. & ABOU-ARAB, T. W. 1983 A two-equation model for two-phase flows. *Phys. Fluids* **26,** 931–938.

ELGHOBASHI, S. & TRUESDELL, G. C. 1993 On the two-way interaction between homogeneous turbulence and dispersed solid particles. 1: turbulence modification. *Phys. Fluids A* **5,** 1790–1801.

ESWARAN, E. & POPE, S. B. 1988 An examination of forcing in direct numerical simulations of turbulence. *Comput. Fluids* **16,** 257–278.

FESSLER, J. R., KULICK, J. D. & EATON, J. K. 1994 Preferential concentration of heavy particles in a turbulent channel flow. Submitted to *Phys. Fluids.*

FICHOT, F., HARSTAD, K. & BELLAN, J. 1993 Unsteady evaporation and combustion of a drop cluster inside a vortex. AIAA 93-0695.

FUNG, J. C. H. & PERKINS, R. J. 1989 Particle trajectories in turbulent flow generated by true-varying random Fourier modes. In *Advances in Turbulence 2* (Edited by FERNHOLZ, H. H. & FIEDLER, H. E.). Springer, New York.

GANAN-CALVO, A. M. & LASHERAS, J. C. 1991 The dynamics and mixing of small spherical particles in a plane, free shear layer. *Phys. Fluids A* **3,** 1207–1217.

GLAWE, D. D. & SAMIMY, M. 1993 Dispersion of solid particles in compressible mixing layers. *J. Propulsion Power* **9,** 83–89.

GORE, R. A. & CROWE, C. T. 1989 Effect of particle size on modulating turbulent intensity. *Int. J. Multiphase Flow* **15,** 279–285.

HANSELL, D., KENNEDY, I. M. & KOLLMAN, W. 1992 A simulation of particle dispersion in a turbulent jet. *Int. J. Multiphase Flow* **18,** 559–576.

HARDALUPAS, Y., TAYLOR, A. M. K. P. & WHITELAW, J. H. 1990 Velocity and size characteristics of liquid-fuelled flames stabilized by a swirl burner. *Proc. R. Soc. Lond.* **A428,** 129–155.

HARDALUPAS, Y., TAYLOR, A. M. K. P. & WHITELAW, J. H. 1992 Particle dispersion in a vertical round sudden-expansion flow. *Proc. R. Soc. Lond.* **A341,** 411–442.

HETSRONI, G. 1989 Particles-turbulence interaction. *Int. J. Multiphase Flow* **15,** 735–746.

HUNT, J. C. R., BUELL, J. C. & WRAY, A. A. 1987 Big whorls carry little whorls. In *Proceedings of the Summer Program 1987,* Center for Turbulence Research, Stanford University, Calif.

HUNT, J. C. R., WRAY, A. A. & MOIN, P. 1988 Eddies, streams and convergence zones in turbulent flows. In *Proc. of the Summer Program 1988,* Center for Turbulence Research, Stanford University, Calif., pp. 193–208.

ISHIMA, T., HISHIDA, K. & MAEDA, M. 1993a Effect of particle residence time on particle dispersion in a plane mixing layer. *Trans. ASME, J. Fluids Engng* **115,** 751–759.

ISHIMA, T., HISHIDA, K. & MAEDA, M. 1993b Particle dispersion in a flow field with vortex shedding behind a pair of vortices. In *ASME FED-Vol 166, Gas–Solid Flows,* pp. 215–220.

KADA, H. & HANRATTY, T. J. 1960 Effects of solids on turbulence in a field. *AIChE Jl* **6,** 624–630.

KAMALU, N., WEN, F., TROUTT, T. R., CROWE, C. T. & CHUNG, J. N. 1988 Particle dispersion by ordered motion in mixing layers. *ASME Cavitation Multiphase Flow Forum FED* **64,** 150–154.

KALLIO, G. A. & REEKS 1989 A numerical simulation of particle deposition in turbulent boundary layers. *Int. J. Multiphase Flow* **15,** 433–446.

KOBAYASHI, H., MASUTANI, S. M., AZUHATA, S., ARASHI, N. & HISHINUMA, Y. 1988 Dispersed phase transport in a plane mixing layer. In *Transport Phenomena in Turbulent Flow,* pp. 433–446. Hemisphere, New York.

KRAICHNAN, R. H. 1970 Diffusion by a random velocity field. *Phys. Fluids* **13,** 22–31.

KULICK, J. D., FESSLER, J. R. & EATON, J. K. 1993 On the interactions between particles and turbulence in a fully-developed channel flow in air. Report MD-66, Department of Mechanical Engineering, Stanford University, Calif.

LAITONE, J. A. 1981 A numerical solution for gas–particles flows at high Reynolds number. *J. appl. Mech.* **48,** 465–471.

LASHERAS, J. C., CHO, J. S. & MAXWORTHY, T. 1986 On the origin and evolution of streamwise vortical structures in a plane, free shear layer. *J. Fluid Mech.* **172,** 231–258.

LAZARO, B. J. & LASHERAS, J. C. 1989 Particle dispersion in a turbulent plane, free shear layer. *Phys. Fluids A* **1,** 1035–1044.

LAZARO, B. J. & LASHERAS, J. C. 1992a Particle dispersion in the developing shear layer. Part 1. Unforced flow. *J. Fluid Mech.* **235,** 143–178.

LAZARO, B. J. & LASHERAS, J. C. 1992b Particle dispersion in the developing shear layer. Part 2. Forced flow. *J. Fluid Mech.* **235,** 143–178.

LILLEY, D. G. 1977 Swirl flows in combustion: a review. *AIAA J.* **15,** 1063–1078.

LONGMIRE, E. K. & ANDERSON, S. L. 1993 Particle–turbulence interactions near solid surfaces. Progress report submitted to EPRI.

LONGMIRE, E. K. & EATON, J. K. 1992 Structure of a particle-laden round jet. *J. Fluid Mech.* **236,** 217–257.

MALLIER, R. & MAXEY, M. 1991 The settling of nonspherical particles in a cellular flow field. *Phys. Fluids A* **3,** 1481–1494.

MAXEY, M. R. & CORRSIN, S. 1986 Gravitational settling of aerosol particles in randomly oriented cellular flow fields. *J. Atmospher. Sci.* **43,** 1112–1134.

MCDONELL, V. G., ADACHI, M. & SAMUELSEN, G. S. 1992 Structure of reacting and non-reacting swirling air-assisted sprays. *Combust. Sci. Technol.* **82,** 225–248.

MCLAUGHLIN, J. B. 1989 Aerosol particle deposition in numerically simulated channel flow. *Phys. Fluids A* **1,** 1211–1224.

MEI, R., ADRIAN, R. J. & HANRATTY, T. J. 1991 Particle dispersion in isotropic turbulence under Stokes drag and Basset force with gravitational settling. *J. Fluid Mech.* **225,** 481–495.

NEUMANN, P. & UMHAUER, H. 1991 Characterization of the spatial distribution state of particles transported by a turbulent gas flow. *Exp. Fluids* **12,** 81–89.

OSEEN, C. 1927 *Neu. Meth. Ergeb. Hydro.* Akademische Verlagsgesellschaft, Leipzig.

PEDINOTTI, S., MARIOTTI, G. & BANERJEE, S. 1992 Direct numerical simulation of particle behavior in the wall region of turbulent flows in horizontal channels. *Int. J. Multiphase Flow* **18,** 927–941.

RASHIDI, M., HETSRONI, G. & BANERJEE, S. 1990 Particle–turbulence interaction in a boundary layer. *Int. J. Multiphase Flow* **16,** 935–949.

REEKS, M. W. 1983 The transport of discrete particles in inhomogeneous turbulence. *J. Aerosol Sci.* **14,** 729–739.

RILEY, J. J. & PATTERSON, G. S. 1974 Diffusion experiments with numerically integrated isotropic turbulence. *Phys. Fluids* **17,** 292–297.

ROBINSON, S. K. 1991 Coherent motions in the turbulent boundary layer. *Ann. Rev. Fluid Mech.* **23,** 601–639.

ROGALLO, R. S. & MOIN, P. 1984 Numerical simulation of turbulent flows. *Ann. Rev. Fluid Mech.* **16,** 99–137.

ROGERS, M. M. & MOIN, P. M. 1987 The structure of the vorticity field in homogeneous flows. *J. Fluid Mech.* **176,** 33–66.

ROUSON, D. W. I. & EATON, J. K. 1994 Direct Lagrangian/Eulerian simulation of solid particles interacting with a turbulent channel flow. In *ASME Intl. Symp. on Numerical Methods for Multiphase Flows*, Lake Tahoe, Nev.

RUDOFF, R. C., BRENA DE LA ROSA, A., SANKAR, S. V. & BACHALO, W. D. 1989 Time analysis of polydisperse sprays in complex turbulent environments. AIAA 89-0052.

RUETSCH, G. R. & MAXEY, M. R. 1992 The evolution of small-scale structures in homogeneous turbulence. *Phys. Fluids A* **4,** 2747–2760.

RUETSCH, G. R. & MEIBURG, E. 1993 On the motion of small spherical bubbles in two-dimensional vortical flows. *Phys. Fluids A* **5,** 2326–2341.

SAMIMY, M. & LELE, S. K. 1991 Motion of particles with inertia in a compressible free shear layer. *Phys. Fluids A* **3,** 1915–1923.

SNYDER, W. H. & LUMLEY, J. L. 1971 Some measurements of particle velocity autocorrelation functions in turbulent flow. *J. Fluid Mech.* **48,** 41–71.

SOMMERFELD, M., ANDO, A. & WENNERBERG, D. 1992 Swirling, particle-laden flows through a pipe expansion. *Trans. of ASME J. Fluids Engng* **114,** 648–656.

SQUIRES, K. D. & EATON, J.K. 1990a Particle response and turbulence modification in isotropic turbulence. *Phys. Fluids A* **2,** 1191–1203.

SQUIRES, K. D. & EATON, J. K. 1990b Measurements of particle dispersion obtained from direct numerical simulations of isotropic turbulence. *J. Fluid Mech.* **226,** 1–35.

SQUIRES, K. D. & EATON, J. K. 1991 Preferential concentration of particles by turbulence. *Phys. Fluids A* **3,** 1169–1178.

SQUIRES, K. D. & EATON, J. K. 1994 Effect of selective modification of turbulence on two-equation models for particle-laden turbulent flows. *ASME J. Fluids Engng.* In press.

STOKES, G. G. 1851 On the effect of internal friction of fluids on the motion of a pendulum. *Trans. Camb. Phil. Soc.* **9,** 8–16 (reprinted in *Mathematics and Physics Papers III*, Cambridge University, 1992).

SUMER, B. M. & DEIGAARD, R. 1981 Particle motions near the bottom in turbulent flow in an open channel. Part 2. *J. Fluid Mech.* **109,** 311–337.

TANG, L., WEN, F., YANG, Y., CROWE, C. T., CHUNG, J. N. & TROUTT, T. R. 1992 Self-organizing particle dispersion mechanism in a plane wake. *Phys. Fluids A* **4,** 2244–2251.

TAYLOR, G. I. 1921 Diffusion by continuous movements. *Proc. R. Soc. Lond. A* **20,** 196–211.

TIO, K., LINAN, A., LASHERAS, J. C. & GANAN-CALVO, A. M. 1993 On the dynamics of buoyant and heavy particles in a periodic Stuart vortex flow. *J. Fluid Mech.* **254,** 671–699.

TORY, E. M., KAMEL, M. T. & CHAN MAN FANG, C. F. 1992 Sedimentation is container size dependent. *Powder Technol.* **73,** 219–238.

UTHUPPAN, J., AGGARWAL, S. K., GRINSTEIN, F. F. & KAILASANATH, K. 1993 Particle dispersion in a transitional axisymmetric jet: a numerical simulation. AIAA 93-0105.

WANG, L. 1992 Dispersion of particles injected nonuniformly in a mixing layer. *Phys. Fluids A* **4,** 1599–1601.

WANG, L. P. & MAXEY, M. R. 1993 Settling velocity and concentration distribution of heavy particles in homogeneous isotropic turbulence. *J. Fluid Mech.* **256,** 27–68.

WELLS, M. R. & STOCK, D. E. 1983 The effects of crossing trajectories on the dispersion of particles in a turbulent flow. *J. Fluid Mech.* **136,** 31–62.

WEN, F., KAMALU, N., CHUNG, J. N., CROWE, C. T. & TROUTT, T. R. 1992 Particle dispersion by vortex structures in plane mixing layers. *Trans. of ASME, J. Fluids Engng* **114,** 657–666.

WICKER, R. B. & EATON, J. K. 1994 Personal communication.

WINANT, C. D. & BROWAND, F. K. 1974 Vortex pairing; mechanisms of mixing layer growth at moderate Reynolds number. *J. Fluid Mech.* **63,** 237–255.

WRAY, A. A. & HUNT, J. C. R. 1989 Algorithms for classification of turbulent structures. In *Proc. IUTAM Topology of Fluid Mechanics*, Cambridge, pp. 95–104.

YANG, Y., CROWE, C. T., CHUNG, J. N. & TROUTT, T. R. 1993 Quantitative study of particle dispersion in a bluff-body wake flow. *ASME FED-Vol. 166, Gas–Solid Flows*, pp. 231–236.

YOUNG, J. B. & HANRATTY, T. D. 1991a Optical studies on the turbulent motion of solid particles in a pipe flow. *J. Fluid Mech.* **231,** 665–688.

YOUNG, J. B. & HANRATTY, T. J. 1991b Trapping of solid particles at a wall in a turbulent flow. *AIChE Jl* **37,** 1529–1536.